A Combined Experimental and Density Functional Theory Investigation of Hydrocarbon Activation at a Cationic Platinum(II) Diimine Aqua Complex under Mild Conditions in a Hydroxylic Solvent

Hanne Heiberg,[1a] Lars Johansson,[1b] Odd Gropen,[1a] Olav B. Ryan,[1c] Ole Swang,[1c] and Mats Tilset*[1b,d]

Contribution from the Department of Chemistry, University of Oslo, P.O. Box 1033 Blindern, N-0315 Oslo, Norway, Department of Chemistry, University of Tromsø, N-9037 Tromsø, Norway, and SINTEF Applied Chemistry, Department of Hydrocarbon Process Chemistry, P.O. Box 124 Blindern, N-0314 Oslo, Norway

Received May 31, 2000

Abstract: Controlled protonolysis of (N^f-N^f)$Pt(CH_3)_2$ (**1**; N^f-N^f = ArN=CMe−CMe=NAr, Ar = 3,5-$(CF_3)_2C_6H_3$) with HBF_4·Et_2O in dichloromethane in the presence of small quantities of water gives the BF_4^- salt of the aqua complex (N^f-N^f)$Pt(CH_3)(H_2O)^+$ (**6**). When dissolved in trifluoroethanol (TFE), **6**(BF_4^-) effects the activation of methane and benzene C−H bonds under very mild conditions. Thus, **6** reacted with benzene in TFE-d_3 at ambient temperature to quantitatively yield (N^f-N^f)$Pt(C_6H_5)(H_2O)^+$ and methane after 2−3 h. The use of C_6D_6 led to multiple incorporation of deuterium into the methane produced and suggests the involvement of methane σ-complex and benzene σ- or π-complex intermediates. When the solution of **6**(BF_4^-) was exposed to $^{13}CH_4$, an exchange reaction produced ca. 50% of (N^f-N^f)$Pt(^{13}CH_3)(H_2O)^+$ and CH_4 after ca. 48 h at 45 °C. The reaction was inhibited by added water, suggesting that water is reversibly lost from **6** before C−H activation takes place. The use of CD_4 resulted in multiple deuterium incorporation into the methane produced, again implying a Pt−methane σ-complex intermediate. Low-temperature protonation of **1** in dichloromethane-d_2 generated observable Pt(IV) hydride species (N^f-N^f)$Pt(CH_3)_2(H)(L)^+$. These decomposed via methane elimination, raising the possibility that the observed C−H activation proceeds by an oxidative addition pathway. The reaction between **6** and CH_4 was investigated by DFT calculations using a model system with the HN=CH−CH=NH ligand. The C−H activation was investigated for oxidative addition and σ-bond metathesis pathways starting from the four-coordinate methane complex (N-N)$Pt(CH_3)(CH_4)^+$. The oxidative addition pathway, thermodynamically uphill by 23 kJ/mol (ZPE-corrected data), was favored by 12 kJ/mol relative to the σ-bond metathesis. When a H_2O ligand was added to the five-coordinate oxidative addition product, the overall oxidative addition reaction was thermodynamically downhill by 33 kJ/mol (partially ZPE-corrected) starting from an H_2O adduct of (N-N)$Pt(CH_3)(CH_4)^+$ with H_2O electrostatically bonded at the diimine moiety. In this case, the oxidative addition pathway was favored by 20 kJ/mol. The calculations indicated that reductive elimination of methane from the six-coordinate (N-N)$Pt(CH_3)_2(H)(H_2O)^+$ with the hydride and H_2O ligands trans disposed occurred in concert with dissociation of the aqua ligand.

Introduction

The direct, selective conversion of alkanes into value-added chemical products has long been a "holy grail" for chemists,[2] and intensified efforts toward this goal have been made by organometallic chemists during the past few years.[3] Shilov and co-workers demonstrated as early as 1969 that transition metal complexes in the form of Pt(II) salts were capable of activating alkane C−H bonds.[4] Some years later, Shilov also reported that catalytic conversion of alkanes (including methane) to mixtures of the corresponding chlorides and alcohols could be achieved by employing aqueous solutions of Pt(II) and Pt(IV) salts.[5] Stoichiometric additions of alkane C−H bonds at highly reactive, coordinatively and electronically unsaturated organotransition metal species such as Cp*Rh(PMe_3), Cp*Ir(PMe_3), and Cp*Ir(CO) were achieved in the 1980s,[6,7] but the conversion

(1) (a) University of Tromsø. (b) University of Oslo. (c) SINTEF. (d) E-mail for corresponding author: mats.tilset@kjemi.uio.no.

(2) Arndtsen, B. A.; Bergman, R. G.; Mobley, T. A.; Peterson, T. H. *Acc. Chem. Res.* **1995**, *28*, 154.

(3) (a) Shilov, A. E.; Shulpin, G. B. *Chem. Rev.* **1997**, *97*, 2879. (b) Stahl, S. S.; Labinger, J. A.; Bercaw, J. E. *Angew. Chem., Int. Ed. Engl.* **1998**, *37*, 2180. (c) Bengali, A. A.; Arndtsen, B. A.; Burger, P. M.; Schultz, R. H.; Weiller, B. H.; Kyle, K. R.; Moore, C. B.; Bergman, R. G. *Pure Appl. Chem.* **1995**, *67*, 281. (d) Crabtree, R. H. *Chem. Rev.* **1995**, *95*, 987. (e) Sen, A. *Acc. Chem. Res.* **1998**, *31*, 550.

(4) Goldshlegger, N. F.; Tyabin, M. B.; Shilov, A. E.; Shteinman, A. A. *Zh. Fiz. Khim.* **1969**, *43*, 2174.

(5) Goldshlegger, N. F.; Eskova, V. V.; Shilov, A. E.; Shteinman, A. A. *Zh. Fiz. Khim.* **1972**, *46*, 1353.

(6) For some early references, see: (a) Janowicz, A. H.; Bergman, R. G. *J. Am. Chem. Soc.* **1982**, *104*, 352. (b) Wax, M. J.; Stryker, M. J.; Buchanan, J. M.; Kovac, C. A.; Bergman, R. G. *J. Am. Chem. Soc.* **1984**, *106*, 1121. (c) Periana, R. A.; Bergman, R. G. *J. Am. Chem. Soc.* **1984**, *106*, 7272. (d) Hoyano, J. K.; Graham, W. A. G. *J. Am. Chem. Soc.* **1982**, *104*, 3723. (e) Jones, W. D.; Feher, F. J. *J. Am. Chem. Soc.* **1982**, *104*, 4240.

(7) Abbreviations: Cp* = (η^5-C_5Me_5; tmeda = tetramethylethylenediamine; Tp′ = hydridotris(3,5-dimethylpyrazolyl)borate; bpym = 2,2′-bipyrimidine; OTf^- = triflate; BAr_f^- = [3,5-$(CF_3)_2C_6H_3]_4B^-$; N^f-N^f = ArN=CMeCMe=NAr with Ar = 3,5-$(CF_3)_2C_6H_3$; TFE = trifluoroethanol.

10.1021/ja0019171 CCC: $19.00
Published on Web 10/21/2000

of the C−H insertion organometallic complexes (eq 1) to organic products R−X has been difficult to achieve, in particular with catalysis in mind. The high air sensitivity of the neutral, low-

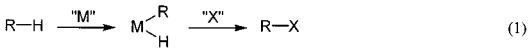

(1)

oxidation-state organometallic complexes constitutes one major problem for the conversion of alkanes to valuable products under oxidizing conditions. Different approaches, some including Pt complexes that may be related to the classical Shilov systems, have now emerged that appear to hold some promise for future developments.

A novel approach to alkane C−H activation and functionalization involves the use of cationic, relatively electrophilic metal complexes. Burger and Bergman[8a] reported that Cp*Ir(PMe_3)(CH_3)(OTf) activates C−H bonds in methane (45 °C, CD_2Cl_2) and a wide variety of other hydrocarbons. Anion exchange with $Na^+BAr_f^-$ in dichloromethane yielded the crystalline salt Cp*Ir(PMe_3)(CH_3)($ClCH_2Cl$)$^+BAr_f^-$, characterized by X-ray crystallography. This salt was shown to activate methane and other hydrocarbon C−H bonds at subambient temperatures in dichloromethane.[8b] The presumed crucial unsaturated intermediate in the C−H activation process, Cp*Ir(PMe_3)(CH_3)$^+$,[8c] is believed to be readily accessible through dissociation of the weakly coordinated dichloromethane and triflate ligands from Cp*Ir(PMe_3)(CH_3)($ClCH_2Cl$)$^+$ and Cp*Ir(PMe_3)(CH_3)(OTf), respectively.

Recent work by the Bercaw and Labinger group[9] has also exploited unsaturated, electrophilic metal centers, in this case based on Pt(II) (with obvious implications for the development of chemistry based on the original work by Shilov). Thus, exchange of labeled $^{13}CH_3$ for CH_3 between (tmeda)Pt^{II}(NC_5F_5)(CH_3)$^+$ and $^{13}CH_4$ was observed in pentafluoropyridine, a solvent of low basicity and coordinating ability, and this demonstrated the activation of methane C−H bonds at Pt.[9b,c] Further demonstrating the potential for alkane activation at Pt complexes, Wick and Goldberg showed through the reaction between (η^2-Tp′)Pt^{II}(CH_3) and various hydrocarbons R−H that it is possible to trap the normally elusive five-coordinated oxidative addition product by intramolecular pyrazole coordination, ultimately producing Pt(IV) complexes (η^3-Tp′)Pt(H)(CH_3)(R).[10] Recently, a remarkable Pt-catalyzed conversion of methane to methyl bisulfate was achieved with the complex (bpym)$PtCl_2$ as a catalyst precursor in concentrated sulfuric acid media.[11] Importantly, the latter system works under oxidizing conditions, an important detail with respect to catalytic functionalization of C−H bonds.

An interesting and common feature in the above examples is the success of employing bidentate nitrogen ligands to obtain Pt(II) complexes that are reactive toward C−H bond activation. We have recently[12] reported a study of the one-electron oxidation reactions of Pt(II) complexes (diimine)Pt(CH_3)$_2$ (diimine = ArN=CH−CH=NAr or ArN=CMe−CMe=NAr, with Ar = *p*-MeC_6H_4 or *p*-$MeOC_6H_4$), in acetonitrile. For the diimine (*p*-$MeOC_6H_4$)N=CH−CH=N(*p*-$MeOC_6H_4$), the oxidation resulted in intermolecular methyl-transfer reactions, giving (diimine)Pt^{IV}(NCMe)(CH_3)$_3^+$ and (diimine)Pt^{II}(NCMe)(CH_3)$^+$. The latter was presumably formed via the intermediacy of (diimine)Pt(CH_3)$^+$, an analogue of the species believed to be responsible for the C−H activation in the (tmeda)Pt^{II} system.[9] In this contribution, we report experimental and theoretical details about the activation of benzene and methane C−H bonds at a related (diimine)Pt aqua complex in a hydroxylic solvent, under mild and neutral conditions.[13]

Results and Discussion

I. Experimental Work. Ligand and Complex Synthesis. We recently described[12] the preparation and electrochemical behavior of a series of (diimine)Pt(CH_3)$_2$ complexes, where diimine = ArN=CH−CH=NAr or ArN=CMe−CMe=NAr, with Ar = *p*-MeC_6H_4 or *p*-$MeOC_6H_4$. The protonation of these (diimine)Pt(CH_3)$_2$ complexes with 1 equiv of HOTf, HBF_4, or $H(Et_2O)_2BAr_f$ in poorly coordinating solvents (dichloromethane-d_2, nitromethane-d_3) immediately generated methane and several unidentified cationic (diimine)Pt(CH_3)$^+$ species that underwent extensive decomposition, as evidenced by the plethora of new signals that appeared in the ^{1}H NMR spectra. The decomposition of the cationic species was accompanied by the formation of additional quantities of CH_4. We tentatively attribute this behavior to a propensity of the in situ-generated (diimine)Pt(CH_3)$^+$ species to undergo intermolecular reactions with the diimine ligands of adjacent Pt complexes, and reasoned that this undesirable degradation might be avoided by appropriate protection of the *N*-aryl groups of the diimine. A 3,5-bis(trifluoromethyl)phenyl-substituted diimine (henceforth to be denoted N^f-N^f) was selected as a new ligand, and this ligand is synthesized in a modest (26%) yield by a modification of methods described for the preparation of other diimines.[14] The corresponding dimethylplatinum complex (N^f-N^f)Pt(CH_3)$_2$ (**1**) is straightforwardly prepared in 91% yield by the reaction of N^f-N^f with $Pt_2(CH_3)_4(\mu\text{-}SMe_2)_2$, a standard preparative route to (diimine)Pt(CH_3)$_2$ complexes.[15] Similarly, the diphenyl analogue (N^f-N^f)Pt(C_6H_5)$_2$ (**2**) can be prepared from Pt(SMe_2)$_2$(C_6H_5)$_2$[16] and N^f-N^f. The ^{1}H and ^{19}F NMR spectra of **1** and **2** (Table 1) are in complete agreement with the anticipated square planar geometry and the overall C_{2v} symmetry of the molecules.

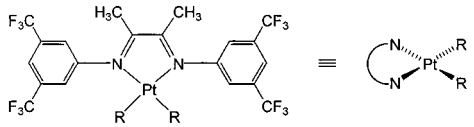

1, R = CH_3
2, R = C_6H_5

In reactive, cationic derivatives of **1**, the two CF_3 groups should serve to sterically as well as electronically protect each aryl ring against electrophilic attack by adjacent Pt species. As an added benefit, it was reasoned that the CF_3 groups also decrease the electron density and thus increase the electrophilicity of the metal center, an effect which might increase the affinity of the putative three-coordinate cationic intermediate (diimine)Pt(CH_3)$^+$ for hydrocarbon C−H bonds. The electronic

(8) (a) Burger, P.; Bergman, R. G. *J. Am. Chem. Soc.* **1993**, *115*, 10462. (b) Arndtsen, B. A.; Bergman, R. G. *Science* **1996**, *270*, 1970. (c) Luecke, H. F.; Bergman, R. G. *J. Am. Chem. Soc.* **1997**, *119*, 11538.

(9) (a) Stahl, S. S.; Labinger, J. A.; Bercaw, J. E. *J. Am. Chem. Soc.* **1996**, *118*, 5961. (b) Holtcamp, M. W.; Labinger, J. A.; Bercaw, J. E. *J. Am. Chem. Soc.* **1997**, *119*, 848. (c) Holtcamp, M. W.; Henling, L. M.; Day, M. W.; Labinger, J. A.; Bercaw, J. E. *Inorg. Chim. Acta* **1998**, *270*, 467.

(10) Wick, D. D.; Goldberg, K. I. *J. Am. Chem. Soc.* **1997**, *119*, 10235.

(11) Periana, R. A.; Taube, J. D.; Gamble, S.; Taube, H.; Satoh, T.; Fujii, H. *Science* **1998**, *280*, 560.

(12) Johansson, L.; Ryan, O. B.; Rømming, C.; Tilset, M. *Organometallics* **1998**, *17*, 3957.

(13) Part of the work has been previously communicated. Johansson, L.; Ryan, O. B.; Tilset, M. *J. Am. Chem. Soc.* **1999**, *121*, 1974.

(14) tom Dieck, H.; Svoboda, M.; Grieser, T. *Z. Naturforsch.* **1981**, *36B*, 823.

(15) Scott, J. D.; Puddephatt, R. J. *Organometallics* **1983**, *2*, 1643.

(16) Hadj-Bagheri, N.; Puddephatt, R. J. *Polyhedron* **1988**, *7*, 2695.

Table 1. Key NMR Data for New Complexes

compound	^{1}H NMR, δ Pt−*Me* ($^2J(^{195}$Pt−H))	diimine−*Me*	aryl−*H* (2,6; 4)	other	^{19}F NMR, δ
free ligand[a]		2.16	7.22; 7.65		−63.50
(N^f-N^f)Pt(CH_3)$_2$ (**1**)[b]	1.14 (87.2)	1.35	7.57; 7.89		−63.14
(N^f-N^f)Pt(C_6H_5)$_2$ (**2**)[b]		1.82	7.26; 7.60	6.42−6.73 (Ph)	−63.21
(N^f-N^f)Pt(CH_3)(NCMe)$^+$ (**3**)[c]	0.71 (74.5)	2.02, 2.13	7.59, 7.74; 8.01, 8.04	2.10 (*Me*CN)	−63.64, −63.41
(N^f-N^f)Pt(C_6H_5)(NCMe)$^+$ (**4**)[c]		2.14, 2.28	7.27, 7.65; 7.81, 8.07	2.01 (*Me*CN); 6.65−6.75 (Ph)	−63.63, −63.37
(N^f-N^f)Pt(CH_3)(OTf) (**5**)[b]	1.07 (74.9)	1.65, 2.01	7.62, 7.71; 7.96, 8.01		−78.48 ($^4J(^{195}$Pt−F) = 14.5 Hz), −63.47, −63.36
(N^f-N^f)Pt(CH_3)(OH_2)$^+$ (**6**)[c]	0.79 (73.3)	1.80, 2.05	7.58, 8.00; 7.71, 8.00		−63.64, −63.52
(N^f-N^f)Pt(CH_3)(OH_2)$^+$ (**6**)[d]	0.69 (73.5)	1.81, 2.07	7.58, 7.96; 7.70, 7.96	6.51 (H_2O)	
(N^f-N^f)Pt(C_6H_5)(OH_2)$^+$ (**7**)[c]		1.91, 2.19	7.29, 7.65; 7.79, 8.05	6.65−6.85 (Ph)	−63.65, −63.48
(N^f-N^f)Pt(CH_3)$_2$(H)(L)$^+$ (**8a**,**b**)	**a**: 0.54 (63.6) **b**: 0.48 (62.9)	2.42 2.37	7.36, 7.92 7.36, 7.71	−26.67 (^1J = 1741 Hz) −26.40 (^1J = 1699 Hz)	

[a] Chloroform-*d*. [b] Dichloromethane-d_2. [c] Trifluoroethanol-d_3. [d] Dichloromethane-d_2 with 250 equiv of TFE.

effect of the ligand is corroborated by the measured reversible electrode potentials for the first ligand-centered reductions of (ArN═CMe−CMe═NAr)Pt(CH_3)$_2$ by cyclic voltammetry in acetonitrile/0.1 M Bu_4NPF_6: Ar = *p*-MeC_6H_4, $E° = -1.75$ V;[12] *p*-MeOC_6H_4, −1.76 V;[12] and 3,5-(CF_3)$_2C_6H_3$, −1.42 V vs Cp_2Fe/Cp_2Fe^+. Admittedly, the electron density at the metal would be better probed through the corresponding presumably metal-centered oxidation potentials. Unfortunately, the oxidation waves for these dimethyl complexes[12] are usually rather ill-defined and poorly reproducible due to fouling of the electrodes by adsorption, and are also chemically irreversible even at voltage scan rates as high as 100 V/s, so thermodynamically meaningful oxidation potential data are not available.

Protonolysis of **1** and **2** with HBF_4·Et_2O in the presence of acetonitrile (eq 2) generates the expected acetonitrile adducts (N^f-N^f)Pt(CH_3)(NCMe)$^+$ (**3**) and (N^f-N^f)Pt(C_6H_5)(NCMe)$^+$ (**4**), presumably via protonation at Pt and reductive elimination of methane and benzene, respectively. The ^{1}H and ^{19}F NMR data

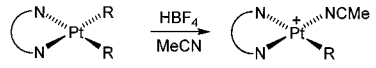

(2)

1, R = CH_3; **2**, R = C_6H_5 — **3**, R = CH_3; **4**, R = C_6H_5

are consistent with the reduced symmetry of **3** and **4** when compared to that of **1** and **2**. Complexes **3** and **4** were prepared to facilitate the indirect identification of other derivatives (vide infra). They are, as expected, found to be rather unreactive with respect to C−H activation chemistry, presumably due to strong binding of the MeCN ligands and thence difficulties with providing the necessary coordination site for substrate binding. For example, **3** reacts slowly with benzene only at elevated temperatures (90 °C) in dichloromethane or nitromethane.

Attempted Synthesis and Isolation of the Triflate Complex (N^f-N^f)Pt(CH_3)(OTf) (5). Having as the ultimate goal an isolable complex that in solution would activate alkane C−H bonds, we attempted to prepare the Pt^{II} triflate complex (N^f-N^f)Pt(CH_3)(OTf) (**5**) by protonolysis of (N^f-N^f)Pt(CH_3)$_2$ (**1**) with 1 equiv of HOTf in dichloromethane (eq 3). An orange solid was

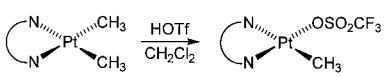

(3)

1 — **5**

obtained after removal of the solvent. The NMR spectra of this solid in dichloromethane-d_2 confirmed that **5** indeed was the major product (ca 90% of isolated mixture). The Pt−CH_3 group shows a diagnostic ^{1}H NMR singlet with ^{195}Pt satellites ($^2J(^{195}$Pt−H) = 74.9 Hz) at δ 1.07 in the ^{1}H NMR spectrum. In the ^{19}F NMR spectrum of **5**, the triflate resonance appears at δ −78.48 (integrating for 3 F; arene CF_3 groups serve as an internal standard). *Most notably, satellites due to coupling from the triflate CF_3 group to ^{195}Pt can clearly be observed* ($^4J(^{195}$Pt−F) = 14.5 Hz). This unambiguously establishes that the triflate group is covalently bonded to the Pt center in solution.[17] As has been pointed out in a review,[18] it is frequently nearly impossible to determine from spectroscopic data (IR, NMR) alone whether a triflate complex exists in the covalently bonded or dissociated form. The possible observation of ^4J(M−F) couplings can be a powerful tool for resolving this ambiguity. It appears that ^{19}F NMR spectroscopy is a surprisingly underutilized tool in the study of organotransition metal triflate complexes.

The triflate complex **5** is rather unstable in dichloromethane at ambient temperature. In the ^{1}H and ^{19}F NMR spectra, the signals for **5** decreased to ca. one-third of their original intensities over a period of 62 h. The degradation of **5** is accompanied by evolution of CH_4 and formation of a brown precipitate. An NMR analysis of the precipitate in acetone-d_6 revealed a complex mixture of unidentifiable compounds. Thus, the decomposition of **5** appears to be less selective than that of the related compound (tmeda)Pt(CH_3)(OEt_2)$^+$(BAr_f^-), which undergoes chloride abstraction in dichloromethane to eventually give the dimeric product [(tmeda)PtCl]$_2^{2+}$(BAr_f^-)$_2$ in a relatively clean reaction.[9b,c] The instability of **5** in dichloromethane contrasts the properties of Bergman's reactive, yet isolable, Cp*Ir(PMe_3)(CH_3)($ClCH_2Cl$)$^+BAr_f^-$ complex.[8b] It is also interesting to note that Kubas and co-workers have recently characterized a stable, cationic Pt^{II} dichloromethane complex,

(17) For other (diimine)Pt^{II}(OTf) and (diimine)Pt^{IV}(OTf) complexes described in the literature, corresponding triflate $^4J(^{195}$Pt−F) coupling constants have, to our knowledge, never been observed or reported. See, for example: (a) Hill, G. F.; Rendina, L. M.; Puddephatt, R. J. *J. Chem. Soc., Dalton Trans.* **1996**, 1809. (b) Hill, G. F.; Yap, G. P. A.; Puddephatt, R. J. *Organometallics* **1999**, *18*, 1408. (c) van Asselt, R.; Rinjberg, E.; Elsevier, C. J. *Organometallics* **1994**, *13*, 706.

(18) (a) Beck, W.; Sünkel, K. *Chem. Rev.* **1988**, *88*, 1405. (b) Strauss, S. H. *Chem. Rev.* **1993**, *93*, 927.

trans-$[(P^iPr_3)_2Pt(H)(ClCH_2Cl)]^+BAr_f^-$.[19] The degradation of **5** in dichloromethane has not been further investigated.

Efforts were made to generate **5** in nitromethane, a relatively poorly coordinating solvent that was hoped to be less reactive than dichloromethane. However, addition of 1 equiv of HOTf to a suspension of **1** in nitromethane-d_3 led to a complex mixture of 3−5 compounds containing the $(N^f\text{-}N^f)Pt(CH_3)^+$ fragment. None of the major species could be identified as **5**, since essentially the same mixture of compounds was obtained when $HBF_4{\cdot}Et_2O$ or $H(Et_2O)_2^+BAr_f^-$ was used instead of HOTf. The aqua complex $(N^f\text{-}N^f)Pt(CH_3)(H_2O)^+BF_4^-$ (**6**(BF_4^-), vide infra) gave similar mixtures in nitromethane-d_3 and remains the only compound in the solution that has been unambiguously identified. It displayed a broad Pt−OH_2 signal at δ 5.8 in the ^{1}H NMR spectrum.[20] The relative amount of the aqua complex increased upon addition of small amounts of water to the solution. Whatever the other species might be, they all contain ligands that are readily displaced, since the addition of acetonitrile quantitatively and instantly yielded the solvento complex **3**.

The great reactivity of **5** toward all solvents in which it is soluble precluded the purification of the material that was isolated from dichloromethane. Traces of water appeared to be a source of the aqua complex in almost any solvent that was used. We decided to investigate this complex more closely. To favor dissociation of the aqua ligand, thereby generating the putative, reactive 14-electron cation $(N^f\text{-}N^f)Pt(CH_3)^+$, a hydroxylic or hydrogen-bonding, yet poorly coordinating, solvent should be used. In this respect, trifluoroethanol (TFE) is a solvent that has been widely used in organic chemistry, in particular in studies of aliphatic nucleophilic substitutions. This solvent is quite strongly ionizing ($\epsilon = 26.7$[21a]) but only poorly nucleophilic.[21b,c] These properties should make it an attractive choice for the exploration of the chemistry of the cationic and electrophilic Pt complexes.

Preparation and Isolation of the Pt(II) Aqua Complex $(N^f\text{-}N^f)Pt(CH_3)(H_2O)^+BF_4^-$ (6(BF_4^-)). The protonation of **1** with $HBF_4{\cdot}Et_2O$ in dichloromethane in the presence of a small amount of water gave an orange powder after workup. The spectroscopic and elemental analysis data of this material are in agreement with the formulation of this species as $(N^f\text{-}N^f)Pt(CH_3)(H_2O)^+BF_4^-$ (**6**(BF_4^-)). The purity was at least 95%

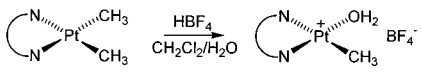

1 **6** (4)

by NMR, sometimes pure within detection limits. The trace impurities may well be due to trace solvent impurities rather than to inherently slightly impure samples. Attempts at recrystallizing **6**(BF_4^-) from various solvents invariably gave materials of poorer purity. In the ^{1}H NMR spectrum, the Pt−CH_3 signal appears at δ 0.79 and displays the expected ^{195}Pt satellites with a coupling constant $^2J(^{195}Pt-H) = 73.3$ Hz, close to the value observed[12] for related (diimine)$Pt(CH_3)(L)^+$ complexes. The aqua ligand could not be observed in TFE-d_3, presumably due to facile H/D exchange with the solvent. The material is only poorly soluble in dichloromethane-d_2 and, in a fashion similar to the triflate complex **5**, undergoes relatively rapid decomposition, generating methane and unidentified organometallic species in this solvent. However, the presence of small amounts of TFE improved the solubility of **6**(BF_4^-) in dichloromethane-d_2 and facilitated an NMR analysis at subambient temperatures. The ^{1}H NMR spectrum in dichloromethane-d_2 with 250 equiv (ca. 2.4 M) of TFE at −20 °C displayed a broadened signal at δ 6.51, integrating for 2 H, which we attribute to coordinated water. This establishes that water is a considerably better ligand than TFE under these conditions.

Electrophilic, coordinatively unsaturated metal fragments commonly coordinate ligands that are usually very weakly coordinating,[18] and we therefore have considered the possibility that the $(N^f\text{-}N^f)Pt(CH_3)^+$ moiety in **6** might be associated with a BF_4^- ligand, rather than water. However, several observations argue against this. First, the ^{19}F NMR spectrum of **6**(BF_4^-) in TFE-d_3 displayed a signal due to BF_4^- at the same chemical shift as $Bu_4N^+BF_4^-$. This would not be expected for a coordinated BF_4^- ligand, whether BF_4^- is rapidly "spinning" or not at the metal.[18] Second, protonation of **1** with HOTf in TFE-d_3 in the presence of water gave a species formulated as **6**(OTf^-) that has a ^{1}H NMR spectrum that is identical to that of **6**(BF_4^-) in TFE-d_3.

C−H Activation of Benzene. In TFE solution, the aqua complex **6**(BF_4^-) underwent facile reaction with the aromatic C−H bonds of benzene and toluene.[22] A quantitative reaction occurred with **6** in the presence of benzene after 2−3 h at ambient temperature, leading to the corresponding phenyl complex $(N^f\text{-}N^f)Pt(C_6H_5)(H_2O)^+$ (**7**) and methane, detected by ^{1}H NMR spectroscopy (eq 5). In comparison, the analogous

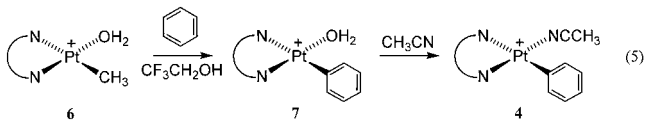

6 **7** **4** (5)

reaction starting with (tmeda)$Pt(CH_3)(NC_5F_5)^+$ required heating for several days in pentafluoropyridine at 85 °C.[9c] The product **7**(BF_4^-) was not isolated but was characterized by NMR spectroscopy. A comparison of the ^{1}H NMR data for **6** and **7** shows that the resonances for the protons on one $C_6H_3(CF_3)_2$ substituent at the diimine have been perturbed more by the substitution of phenyl for methyl than the other, possibly as a result of ring current effects caused by close proximity of phenyl and one $C_6H_3(CF_3)_2$ group. Addition of acetonitrile to the solution after complete conversion to **7** caused the immediate and quantitative replacement of the aqua ligand to yield $(N^f\text{-}N^f)Pt(C_6H_5)(NCMe)^+$ (**4**). The spectroscopic data for **4** thus obtained were identical to those of an authentic sample, prepared as the BF_4^- salt as described earlier.

When **6**(BF_4^-) was treated with C_6D_6 in TFE-d_3, the ^{1}H NMR spectrum revealed multiple incorporation of deuterium in the methane that was generated. Thus, well-resolved and characteristic signals were found for the CH_3D, CH_2D_2, and CHD_3 isotopomers. Similar observations of multiple isotope incorporation were reported for the analogous reaction between (tmeda)$Pt(CH_3)(NC_6F_5)^+$ and C_6D_6,[9] as well as in related reactions with other metals.[23] The multiple H/D exchange into the methane is most readily explained in terms of the reaction steps shown in Scheme 1. (A σ-bond metathesis pathway in which the H/D exchange takes place directly between the η^2-benzene and σ-methane complexes without the intervention of the five-

(19) Butts, M. D.; Scott, B. L.; Kubas, G. J. *J. Am. Chem. Soc.* **1996**, *118*, 11831.

(20) Although the nitromethane-d_3 was carefully purified and dried prior to the reaction, traces of water were always observed in the solutions.

(21) (a) Evans, D. F.; McElroy, M. I. *J. Soln. Chem.* **1975**, *5*, 405. (b) Schadt, F. L.; Bentley, T. W.; Schleyer, P. v. R. *J. Am. Chem. Soc.* **1976**, *98*, 7667. (c) Lowry, T. H.; Richardson, K. S. *Mechanism and Theory in Organic Chemistry*, 3rd ed.; Harper and Row: New York, 1987; pp 335−340.

(22) Details about the reactions with aromatic substrates will be reported elsewhere. See also ref 24.

Scheme 1

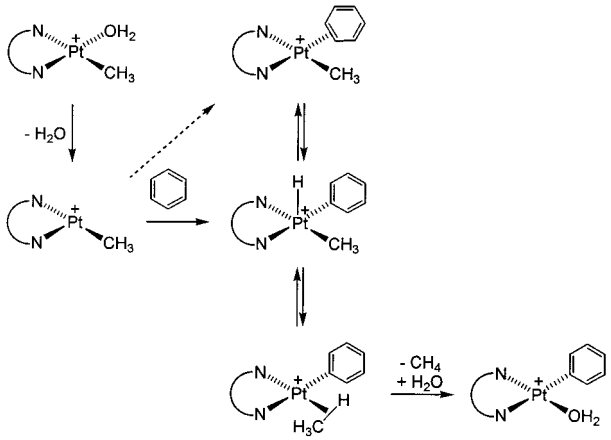

coordinate oxidative addition product might also be devised; aspects of this will be addressed for methane activation in the theoretical part of this paper.) A dynamic equilibrium exists between $(N^f\text{-}N^f)Pt^{II}(CH_3)(\eta^2\text{-benzene})^+$, $(N^f\text{-}N^f)Pt^{IV}(H)(CH_3)(C_6H_5)^+$, and $(N^f\text{-}N^f)Pt^{II}(\sigma\text{-}CH_4)(C_6H_5)^+$ intermediates, all of which are accessible after exchange of benzene for water in **6**. The η^2-benzene complex, which in principle may be η^2(C,H) or η^2(C,C) coordinated,[24] may or may not be an intermediate in the oxidative addition of benzene, but must be involved in the exchange process. Provided that "rotation" of the η^2-C_6H_6 and σ-CH_4 ligands at the respective Pt centers, as well as insertion of Pt into the C−H bonds and the reverse process, are rapid relative to the rate of methane and benzene dissociation, the multiple D incorporation is nicely explained.[25]

C−H Activation of Methane. Encouraged by the above evidence for a methane σ-complex intermediate in the benzene C−H activation, we investigated the possibility that **6** might also activate methane C−H bonds. Indeed, it was found that methane C−H activation occurred under unusually mild conditions. Thus, a solution of **6**(BF_4^-) in TFE-d_3 was sealed under 20−25 bar of $^{13}CH_4$ in an NMR tube. By ^{1}H NMR integration, ca. 20 equiv of $^{13}CH_4$ was present in solution. Unambiguous evidence for methane C−H activation was found during a 2-day period at 45 °C (eq 6). The exchange of $^{13}CH_3$ for the unlabeled

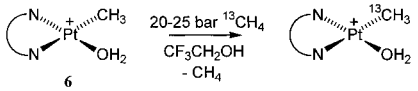

(6)

CH_3 ligand in **6** was readily seen by ^{1}H and $^{13}C\{^1H\}$ NMR spectroscopy. The ^{1}H NMR Pt−CH_3 singlet at δ 0.79, accompanied by ^{195}Pt satellites, was gradually replaced by a doublet ($^1J(^{13}C-H) = 129$ Hz) centered at the same chemical shift. This doublet, as expected, was also accompanied by ^{195}Pt satellites. In the $^{13}C\{^1H\}$ NMR spectrum, the Pt−CH_3 resonance at δ −10.2, as well as its ^{195}Pt satellites ($^1J(^{195}Pt-CH_3) = 744$ Hz), grew in intensity. After a reaction time of 45 h, ^{1}H NMR integration of doublet vs singlet intensity indicated that the extent of $^{13}CH_3$ incorporation was 43% of the total Pt−CH_3 present as **6**. The reaction was accompanied by slow decomposition of **6**, evidenced by the precipitation of a red material that remains unidentified. This decomposition occurred to the same extent (ca. 20%) in the absence of methane. Decomposition might therefore be related to a reaction preceding the C−H activation, rather than to the activation process itself. There was no visible formation of platinum black during the reaction.

The C−H activation at **6** is likely to occur by C−H addition at a formally three-coordinate T-shaped intermediate, $(N^f\text{-}N^f)Pt(CH_3)^+$, that would result from water dissociation from **6**. Support for this hypothesis was obtained when the reaction of **6**(BF_4^-) with $^{13}CH_4$ in TFE-d_3 was performed in the presence of water. With ca. 11 equiv of water added to the reaction medium (reaction conditions were otherwise identical to those used above), it was found that only 24% of $^{13}CH_3$ had been incorporated into **6** after 48 h. Thus, the reaction rate was only half of that found with no water added. This is in agreement with a preequilibrium dissociative mechanism to give a reactive three-coordinate intermediate. However, equally consistent with the observed inhibition is a preequilibrium associative substitution of TFE for H_2O followed by associative replacement of TFE by CH_4.[26] Such a mechanism appears to be involved in the benzene activation by a related complex.[24] The decomposition of **6** was also in part inhibited by the presence of water, amounting to ca. 5% with 11 equiv of water. Therefore, the decomposition may also be a consequence of the initial formation the three-coordinate species or other intermediate(s) en route to the methane σ-complex.

Finally, the reaction between **6** and methane was probed using CD_4 instead of CH_4. Under conditions identical to those used above, a gradual incorporation of deuterium into the Pt−methyl group (giving rise to Pt−$CH_{3-n}D_n$ resonances) was observed in the ^{1}H NMR spectrum. At the same time, signals due to methane, initially absent, appeared. The spectrum showed that the H-containing methane was present as CH_3D, CH_2D_2, and CHD_3 isotopomers. Small amounts of CH_4 were also observed, presumably due to decomposition of **6** (vide supra). The methane isotopomer mixture was observed even at early stages of the reaction. Since a large excess of CD_4 was used, this must mean that *multiple H/D exchange must take place for each C−D activation event that takes place*. In analogy with the observations discussed for the benzene C−H activation earlier, this is most readily explained by the presence of methane σ-complexes as intermediates in the exchange process. The H/D exchange might occur via the oxidative addition pathway (Scheme 2) or by direct H transfer between σ-bonded methane and the methyl group without a discrete oxidative addition product. This will be discussed in the theoretical part that follows. It is interesting to note that multiple H/D exchange into alkanes was also observed by the Shilov group.[4]

Protonolysis of $(N^f\text{-}N^f)Pt(CH_3)_2$ (1) at Low Temperature. The multiple deuterium incorporation into the methane in the above reaction between **6** and CD_4 implies that the H/D

(23) See, for example: (a) Mobley, T. A.; Schade, C.; Bergman, R. G. *J. Am. Chem. Soc.* **1995**, *117*, 7822. (b) Gould, G. L.; Heinekey, D. M. *J. Am. Chem. Soc.* **1989**, *111*, 5502. (c) Wang, C.; Ziller, J. W.; Flood, T. C. *J. Am. Chem. Soc.* **1995**, *117*, 1647. (d) Bullock, R. M.; Headford, C. E. L.; Hennessy, K. M.; Kegley, S. E.; Norton, J. R. *J. Am. Chem. Soc.* **1989**, *111*, 3897. (e) Buchanan, J. M.; Stryker, J. M.; Bergman, R. G. *J. Am. Chem. Soc.* **1986**, *108*, 1537. (f) Parkin, G.; Bercaw, J. E. *Organometallics* **1989**, *8*, 1172. (g) Wick, D. D.; Reynolds, K. A.; Jones, W. D. *J. Am. Chem. Soc.* **1999**, *121*, 3974.

(24) Evidence for an η^2(C,C)-coordinated Pt(II) benzene complex in a related system is described elsewhere. Johansson, L.; Tilset, M.; Labinger, J. A.; Bercaw, J. E. *J. Am. Chem. Soc.* **2000**, *122*, 10845−10854.

(25) As pointed out by a reviewer, the experiment does not demonstrate that all D incorporation into the methyl group comes from the same C_6D_6 molecule, but might arise from multiple oxidative addition/reductive elimination events of different C_6D_6 molecules without the involvement of a discrete π-benzene complex. This would imply that benzene loss from the $(N^f\text{-}N^f)Pt(H)(CH_3)(C_6H_5)^+$ system is much more facile than methane loss. This is contrary to observations in related systems (ref 24).

(26) Associative mechanisms have been reported for solvent-exchange reactions at $(L\text{-}L)Pt(CH_3)(DMSO)^+$ species (L-L = various chelating diimines and diamines). Romeo, R.; Scolaro, L. M.; Nastasi, N.; Arena, G. *Inorg Chem*. **1996**, *35*, 5087.

Scheme 2

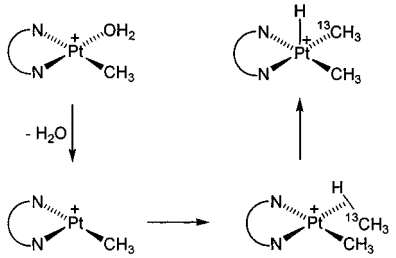

Scheme 3

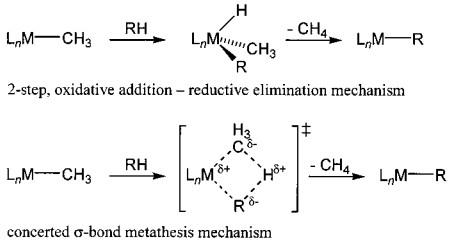

scrambling process must be rapid relative to the rate of methane elimination from the methane σ-complex. This suggests that *if* it is possible to generate any of the intermediates involved in this scrambling process at low temperature, they might have a sufficient stability and lifetime to be observable by NMR. Obviously, it would be desirable to perform such an experiment in the actual TFE solvent system used in the C−H activation reactions. However, due to the high freezing point of TFE (−45 °C) and poor solubility of **1** in this solvent, we decided to perform the experiment in a dichloromethane/ether mixture. An NMR tube containing **1** dissolved in dichloromethane-d_2 was cooled to −78 °C, whereupon 2 equiv of $HBF_4 \cdot Et_2O$ dissolved in a small amount of ether and dichloromethane-d_2 was added. A color change from dark purple to pale yellow was immediately observed. ^{1}H NMR analysis of the yellow solution at −70 °C revealed clean formation of two Pt(IV) hydride species in a ca. 2:1 ratio. The characteristic hydride signals appeared far upfield (δ −26.67 and −26.40) with corresponding Pt satellites $^1J(^{195}\text{Pt}-\text{H})$ of 1741 and 1699 Hz. Furthermore, two methyl signals were found at δ 0.54 and 0.48 with $^2J(^{195}\text{Pt}-\text{H}) = 63.6$ and 62.9 Hz, respectively. These data suggest that both compounds can be formulated as $(N^f\text{-}N^f)Pt^{IV}(CH_3)_2(H)(L)^+$ species (**8a** and **8b**), with the hydride occupying one apical position. We presume that the two species differ in having different stabilizing two-electron donors L coordinated to Pt trans to the hydride. The identity of these could not be determined from the NMR spectra. Above ca. −40 °C, elimination of methane from the species **8a** and **8b** with concurrent formation of unidentified organometallic products was observed. No other intermediates could be detected prior to methane loss. If we assume that this result applies to the current TFE system as well, it suggests that a Pt(IV) hydride species is the energetically most stable of the intermediates involved in the H/D scrambling process discussed above.

II. Theoretical Work. Mechanistic Considerations. Two mechanisms are commonly considered when C−H bond activation reactions at the transition metal are discussed (Scheme 3). The oxidative addition pathway is observed for C−H activation at relatively low-oxidation-state, late-transition-metal centers. The other alternative is the σ-bond metathesis. By this mechanism, C−H activation occurs in a concerted fashion via a four-center, four-electron transition state. This mechanism is observed for early, typically d^0 metals that have no d electrons available for the oxidative addition. When C−H activation at late, cationic metal centers was first discovered with Bergman's $Cp^*Ir(PMe_3)(CH_3)^+$ system, it was immediately realized that an ambiguity existed regarding the mechanism. Although d electrons, as well as the Ir(V) oxidation state (somewhat unusual but far from unprecedented[27] in organometallic chemistry), needed for an oxidative addition pathway were available, it was felt that the cationic 16-electron Ir(III) complex might be sufficiently electrophilic for a σ-bond metathesis pathway to be viable. Since the discovery of this C−H activation process, a number of theoretical contributions have addressed this problem for C−H activation at cationic, late metal centers.

DFT (B3LYP/LANL2DZ)[28a] and ab initio (QCISD/MP2/LANL2DZ)[28b] calculations for methane activation using $CpIr(PH_3)(CH_3)^+$ as a model strongly favored the oxidative addition pathway. A four-center adduct or transition state for a σ-bond metathesis pathway could not be located, and strong doubt was expressed about the feasibility of this mechanism. The two investigations gave very similar results. A methane σ-complex was located 4 and 29 kJ/mol below the energies of the reactants, respectively, and a 48 vs 54 kJ/mol barrier separated this complex from the Ir(V) oxidative addition intermediate, which was located 14 vs 4 kJ/mol higher in energy than the reactants.[28a,b]

C−H activation at cationic Pt centers has also received considerable attention from a theoretical point of view. Hill and Puddephatt[29a] used extended Hückel MO and DFT calculations on the reductive elimination of methane from the five-coordinate model complexes $L_2Pt(H)(CH_3)_2^+$, yielding the methane σ-complexes $L_2Pt(CH_3)(CH_4)^+$ (L = NH_3 or PH_3). The possibility that a $Pt-CH_3/CH_4$ exchange might occur by a σ-bond metathesis pathway was not addressed. Siegbahn and Crabtree[29b] modeled the solvent effect on the Shilov reaction of $PtCl_2$ in water; a σ-bond metathesis-like activation of methane was favored in which a coordinated Cl ligand accepts a proton from a coordinated methane molecule. However, an oxidative addition pathway was not ruled out.

Hush and co-workers[29c] investigated possible mechanisms for the catalytic C−H activation and functionalization by the Pt(bpym) system of Periana et al.[11] The *cis*-diammine system was used as a model, and the solvent (concentrated H_2SO_4) was included by a dielectric continuum method and explicit inclusion of solvento species (coordinated HSO_4^- and H_2SO_4) in the calculations. It was concluded, on thermochemical grounds exclusively, that the crucial C−H activation step is likely to proceed by an electrophilic mechanism rather than by an oxidative addition pathway. However, the validity of these results was somewhat questionable because (a) no transition states and corresponding energies were calculated for either mechanism, and (b) for the hydridoalkyl Pt(IV) intermediates of the oxidative addition pathway, only isomers with a trans (diaxial) relationship between the oxidatively added hydride and

(27) Alaimo, P. J.; Bergman, R. G. *Organometallics* **1999**, *18*, 2707 and references cited.

(28) (a) Strout, D. L.; Zaric, S.; Niu, S.; Hall, M. B. *J. Am. Chem. Soc.* **1996**, *118*, 6068. (b) Su, M.-D.; Chu, S.-Y. *J. Am. Chem. Soc.* **1997**, *119*, 5373. (c) Hinderling, C.; Feichtinger, D.; Plattner, D. A.; Chen, P. *J. Am. Chem. Soc.* **1997**, *119*, 10793. (d) Niu, S.; Hall, M. B. *J. Am. Chem. Soc.* **1998**, *120*, 6169. (e) Niu, S.; Zaric, S.; Bayse, C. A.; Strout, D. L.; Hall, M. B. *Organometallics* **1998**, *17*, 5139. (f) Niu, S.; Hall, M. B. *J. Am. Chem. Soc.* **1999**, *121*, 3992.

(29) (a) Hill, G. S.; Puddephatt, R. J. *Organometallics* **1998**, *17*, 1478. (b) Siegbahn, P. E. M.; Crabtree, R. H. *J. Am. Chem. Soc.* **1996**, *118*, 4442. (c) Mylvaganam, K.; Bacskay, G. B.; Hush, N. S. *J. Am. Chem. Soc.* **1999**, *121*, 4633. (d) Mylvaganam, K.; Bacskay, G. B.; Hush, N. S. *J. Am. Chem. Soc.* **2000**, *122*, 2041. (e) Bartlett, K. L.; Goldberg, K. I.; Borden, W. T. *J. Am. Chem. Soc.* **2000**, *122*, 1456. (f) Heiberg, H.; Swang, O.; Ryan, O. B.; Gropen, O. *J. Phys. Chem. A* **1999**, *103*, 10004.

methyl groups were considered. The cis (axial, equatorial) analogues would be more relevant in particular if a concerted oxidative addition occurs. This was corroborated by a recent extended and revised study by the Hush group[29d] and will also be evident from our results.

Recently, Bartlett, Goldberg, and Borden[29e] presented a detailed theoretical investigation of reductive elimination of alkanes from Pt(II) and Pt(IV) hydridoalkyl complexes. The cationic five-coordinate complex *cis*-$(PH_3)_2Pt(Cl)(CH_3)(H)^+$ was found to undergo exothermic elimination with a very low activation barrier of 4 kJ/mol (B3LYP) to yield a σ-complex in which methane is bonded to the Pt center with a bond energy of 40 kJ/mol.

Some of us recently reported[29f] DFT calculations on $Pt-CH_3/CH_4$ exchange at $(H_2NCH_2CH_2NH_2)Pt(CH_3)^+$, a model for Bercaw and Labinger's $(tmeda)Pt(CH_3)^+$ system. An oxidative addition pathway was strongly favored in this case. To shed light also on the C−H activation at the $(N^f\text{-}N^f)Pt(CH_3)^+$ system, we report here an investigation of the reaction mechanism with quantum chemical methods based on density functional theory (DFT).

Selection of a Suitable Model System for Calculations. The structure of the Pt complex (*p*-$MeOC_6H_4-N{=}CH-CH{=}N-C_6H_4-p$-OMe)$Pt(CH_3)_2$ was calculated with DFT methods[30] (see the Experimental Section for computational details). The *p*-$MeOC_6H_4$ substituent was employed for the full-scale system because the X-ray crystal structure of this Pt complex has been reported,[12] and so its geometry can be compared with the calculated geometry. Gratifyingly, the X-ray crystallographic data and the computationally optimized geometry were found to be in excellent agreement. The differences between observed and calculated geometries were typically less than 0.01 Å for bond distances and less than 2° for bond angles (maximum deviations were 0.02 Å and 4°).

The Pt complexes that were actually used in the experiments are too large for the desired quantum chemical study of the entire C−H bond activation mechanism. The process was therefore modeled with a smaller diimine ligand at the Pt center. The molecular model that was used (the simplest possible—with only H substituents on the diimine!) was chosen after testing six models with different diimine ligands, $X-N{=}C(Y)-C(Y){=}N-X$, where X = $CH{=}CH_2$, CH_3, or H, and Y = CH_3 or H. The reaction energies for several relevant reactions were calculated with DFT methods for the full-sized Pt complex (X = *p*-$MeOC_6H_4$)[30] and used to test the relevance of the six models. The reaction energies that were obtained with models with X or Y ≠ H were not significantly better than those obtained with X and Y = H when compared with the *p*-$MeOC_6H_4$ system, and the smallest molecular model, with X and Y = H, was therefore chosen for the theoretical investigation of the reaction mechanism. The substitution of hydrogen for an aryl substituent at the diimine is a rather dramatic simplification. However, it should be pointed out that the aryl rings are not coplanar with the Pt−diimine plane, and therefore π-overlap between the metal−diimine ring and the aryl rings should be of reduced importance. The optimized geometry of the simple model agreed well with the pertinent bond lengths and angles in the X-ray crystal structure for (*p*-$MeOC_6H_4-N{=}CH-CH{=}N-C_6H_4-p$-OMe)$Pt(CH_3)_2$, as well as with the calculated geometry for this full-size complex. The differences in bond distances and angles between the simple model and the X-ray crystallographic data are typically 0−0.01 Å and 2°. The maximum deviation of 0.05 Å was found in one of the Pt−N bonds, while the other Pt−N bond distance differed by only 0.02 Å. This is caused by the model having a C_{2v} symmetry; a difference of 0.03 Å was found in the Pt−N bond lengths in the crystal structure data. These small differences in Pt−N bond lengths may be due to crystal packing effects. With these considerations, the following calculations were done on the $(HN{=}CH-CH{=}NH)Pt$ system, henceforth to be abbreviated as (N-N)Pt.

Table 2. Calculated Energies for Pt Structures[30]

complex	relative energy (kJ/mol) without ZPE	with ZPE
(**A**) $(N\text{-}N)Pt(CH_3)^+$	99	92[a]
(**B**) $(N\text{-}N)Pt(CH_3)(H_2O)^+$	−59	
(**C**) $(N\text{-}N)Pt(CH_3)(TFE)^+$	−49	
(**D**) $(N\text{-}N)Pt(CH_3)(CH_4)^+$	0	0[a]
(**E**) *ax*-$(N\text{-}N)Pt(CH_3)_2(H)^+$	29	23[a]
(**F**) *eq*-$(N\text{-}N)Pt(CH_3)_2(H)^+$	30	29[a]
(**G**) *ax*-$(N\text{-}N)Pt(CH_3)_2(H)(H_2O)^+$	−58	−64[b]
(**H**) *ax*-$(N\text{-}N)Pt(CH_3)_2(H)(TFE)^+$	−49	−55[b]
(**I**) $(N\text{-}N)Pt(CH_3)(CH_4)^+$ OA#	40	33[a]
(**J**) $(N\text{-}N)Pt(CH_3)(CH_4)^+$ SB#	50	44[a]
(**K**) $(N\text{-}N)Pt(CH_3)(CH_4)(H_2O)^+$	−30	
(**L**) $(N\text{-}N)Pt(CH_3)(CH_4)(TFE)^+$	−27	
(**M**) $(N\text{-}N)Pt(CH_3)(CH_4)(H_2O)^+$ OA#	4	−4[b]
(**N**) $(N\text{-}N)Pt(CH_3)(CH_4)(TFE)^+$ OA#	9	2[b]

[a] ZPE from calculations on the full model complex. [b] Estimated by assuming the same ZPE corrections to solvent-associated species as to the corresponding species without solvents.

Calculations of Relevant Ground-State Species with DFT Methods. Calculations on relevant ground-state species were first performed, largely using DFT methods. The search for and calculation of transition-state structures for the oxidative addition and σ-bond metathesis mechanisms were then undertaken. Table 2 summarizes calculated energies,[31] and Table 3 summarizes key geometrical features for the ground-state complexes as well as transition states (vide infra). An overview of the calculated structures is depicted in Figure 1. In the following, energies include zero-point energy (ZPE) corrections unless otherwise stated. ZPE corrections given for systems containing solvent molecules are estimated by applying the corresponding ZPE corrections of the solvent-free species.[30]

The Three- and Four-Coordinate Cations $(N\text{-}N)Pt(CH_3)(L)^+$ (L = Vacant Site, TFE, H_2O, or CH_4). The cation $(N\text{-}N)Pt(CH_3)^+$ (**A**) is a model for the three-coordinate species that might be responsible for the C−H activation process. The C−H activation of methane takes place in a TFE solution containing a small amount of water. Cationic square planar Pt(II) complexes $(N^f\text{-}N^f)Pt(CH_3)(L)^+$ (L = H_2O, TFE) are likely present. The NMR results indicate that water occupies the empty site of $(N^f\text{-}N^f)Pt(CH_3)^+$ most of the time; we have no spectroscopic evidence for the existence of the corresponding TFE adduct. The calculations show that the bond strengths between the $(N\text{-}N)Pt(CH_3)^+$ moiety and L are 158 and 149 kJ/mol for L = H_2O (**B**) and TFE (**C**), respectively. Steric and electronic factors may both contribute to the weaker bond to TFE.

The Pt(II)−methane σ-complex $(N^f\text{-}N^f)Pt(CH_3)(\sigma\text{-}CH_4)^+$ is a likely intermediate in the C−H activation process.[9] The intermediacy of such a species provides a straightforward explanation for the occurrence of multiple H/D exchange into

(30) Calculations of vibrational frequencies for the optimized structures of the full-size molecules and model complexes that contain solvent molecules have not been performed, for obvious reasons of computational economy. Zero-point energy corrections are therefore not available.

(31) All energies are given for assemblies containing one each of $(N\text{-}N)Pt(CH_3)^+$, H_2O, CH_4, and TFE in order to be directly comparable. For example, the energy of $(N\text{-}N)Pt(CH_3)(H_2O)^+$ implicitly includes the energies of one molecule each of TFE and methane separated at infinite distance.

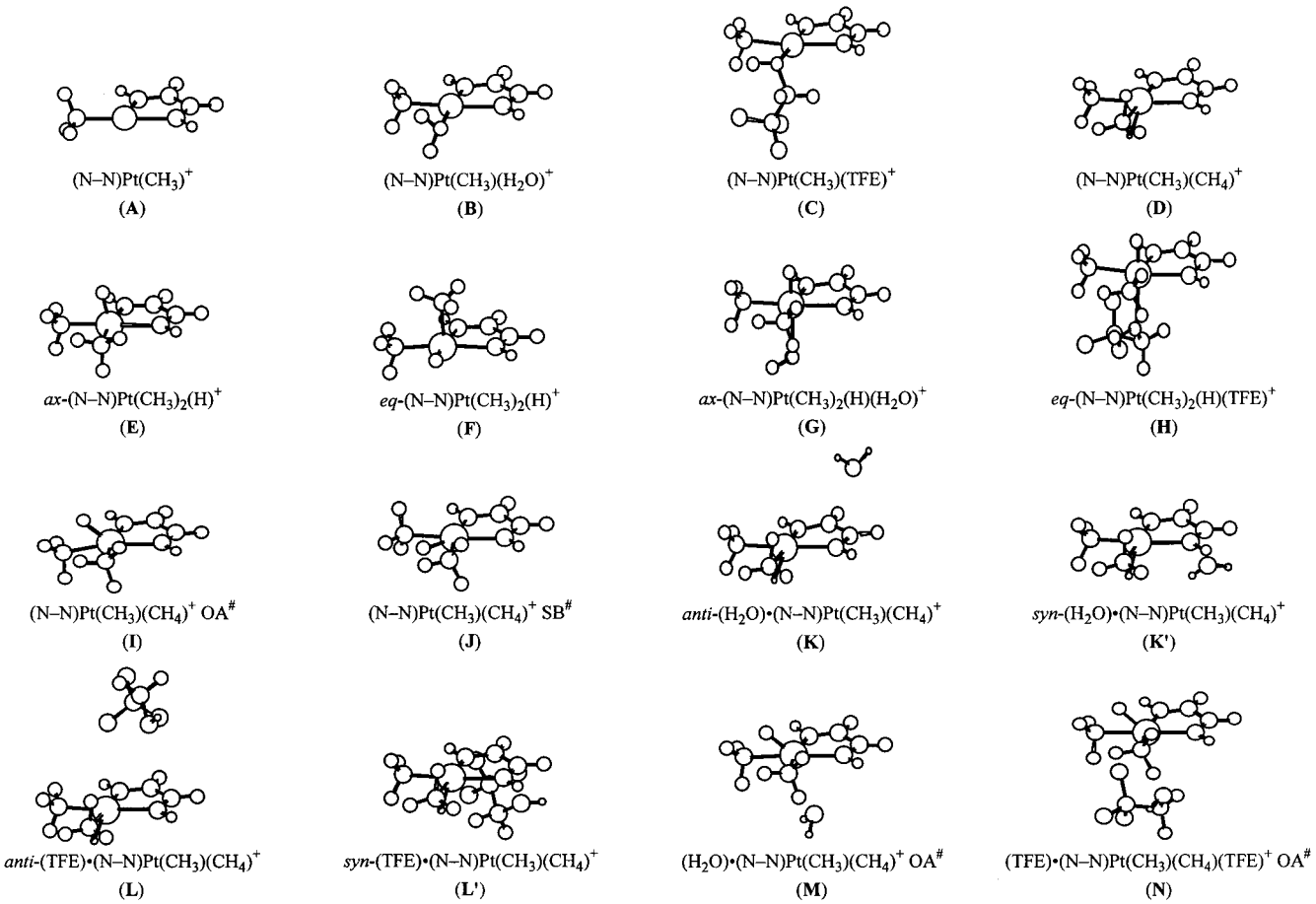

Figure 1. Calculated structures of relevance to the methane C−H activation reaction. See footnote *a* to Table 3 for atom numbering system.

Table 3. Calculated Bond Distances (Å) and Angles (Deg) for Pt Structures[a]

complex	Pt−H(1)	H(1)−C(1)	Pt−C(1)	Pt−C(2)	Pt−N(1)	Pt−N(2)	Pt−O	H(1)−Pt−C(1)	Pt−C(1)−H(1)
(**A**) (N-N)Pt$(CH_3)^+$				2.00	1.93	2.16			
(**B**) (N-N)Pt$(CH_3)(H_2O)^+$				2.04	1.95	2.15	2.13		
(**C**) (N-N)Pt(CH_3)(TFE)$^+$				2.04	1.94	2.16	2.12		
(**D**) (N-N)Pt$(CH_3)(CH_4)^+$	1.84	1.16	2.34	2.04	1.96	2.16		29	51
(**E**) *ax*-(N-N)Pt$(CH_3)_2(H)^+$	1.51	2.42	2.04	2.04	2.19	2.19		84	38
(**F**) *eq*-(N-N)Pt$(CH_3)_2(H)^+$	1.53	2.43	2.07	2.03	2.22	2.19		84	39
(**G**) *ax*-(N-N)Pt$(CH_3)_2(H)(H_2O)^+$	1.51	2.43	2.05	2.05	2.17	2.19	2.34	85	38
(**H**) *ax*-(N-N)Pt$(CH_3)_2(H)$(TFE)$^+$	1.51	2.41	2.05	2.05	2.18	2.18	2.36	84	38
(**I**) (N-N)Pt$(CH_3)(CH_4)^+$ OA#	1.54	1.73	2.11	2.04	2.13	2.17		54	46
(**J**) (N-N)Pt$(CH_3)(CH_4)^+$ SB#	1.59	1.56	2.14	2.14	2.08	2.08		47	48
(**K**) (N-N)Pt$(CH_3)(CH_4)(H_2O)^+$	1.82	1.16	2.36	2.04	1.97	2.16	4.50	29	49
(**L**) (N-N)Pt$(CH_3)(CH_4)$(TFE)$^+$	1.83	1.16	2.35	2.04	1.96	2.16	4.03	29	49
(**M**) (N-N)Pt$(CH_3)(CH_4)(H_2O)^+$ OA#	1.56	1.53	2.14	2.05	2.07	2.16	2.84	46	47
(**N**) (N-N)Pt$(CH_3)(CH_4)$(TFE)$^+$ OA#	1.55	1.56	2.13	2.05	2.08	2.16	2.90	47	47

[a] The following numbering system has been used (see structure, below): H(1), hydride or bridging H in σ-CH_4 complexes; C(1), carbon of σ-CH_4 ligand or of methyl group derived from this ligand; C(2), carbon of methyl ligand; N(1), diimine cis to original methyl; N(2), diimine N trans to original methyl.

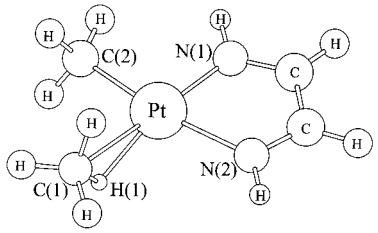

CD_4. Alkane σ-complexes have rarely been directly observed,[32,33] but a large body of evidence strongly implies their existence.[34] Calculations on (N-N)Pt$(CH_3)(CH_4)^+$ (**D**) were done with and without ZPE corrections. The non-ZPE results show

(32) For a recent report of an X-ray structure of a (porphyrin)Fe^{II}(σ-alkane) complex, see: Evans, D. R.; Drovetskaya, T.; Bau, R.; Reed, C. A.; Boyd, P. D. W. *J. Am. Chem. Soc.* **1997**, *119*, 3633.

(33) For a recent account of the direct observation of a Re(I) cyclopentane complex, see: Geftakis, S.; Ball, G. E. *J. Am. Chem. Soc.* **1998**, *120*, 9953; **1999**, *121*, 6336 (addendum).

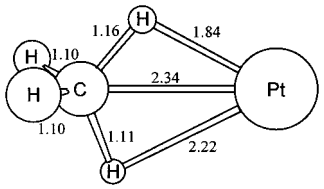

Figure 2. Coordination of the CH_4 ligand at Pt in (N-N)Pt$(CH_3)(CH_4)^+$ (**D**).

that methane binds in what has been termed an η^3(H,C,H)[29a] or η^2(H,C)[35] mode (the latter will be adopted by us) to Pt in the σ-complex, with a non-ZPE-corrected bond energy of 99 kJ/mol. The methane in this complex, shown in a side-on view in Figure 2, is coordinated via two C−H σ-bonds with the H−C−H plane perpendicular to the equatorial plane at Pt and has one elongated C−H bond (1.16 Å, compared to 1.10 Å in free methane). The two Pt−H distances are 1.84 and 2.22 Å, respectively, and the H−C−H angle has opened up to 120°. The calculated vibrational frequency for the activated C−H bond is reduced by 592 cm^{-1} relative to the asymmetric C−H vibration in free methane. The Pt−N bond trans to CH_3 (2.16 Å) is longer than the one trans to CH_4 (1.96 Å), reflecting the greater trans influence of the methyl ligand. The geometry and trends in bond distances closely resemble those calculated for $(H_2NCH_2CH_2NH_2)Pt(CH_3)(CH_4)^+$ [29f] and *cis*-$(NH_3)_2Pt(CH_3)(CH_4)^+$,[29a] with slight differences in the metric parameters.

The CH_4 ligand in **D** appears to undergo a facile "rotation" within the σ-complex via a symmetrical η^2(H,H) structure to form a reoriented η^2(H,C)-bonded ligand. The calculations indicate that the symmetrical structure is a transition state separating two η^2(H,C) minima with a barrier of only 0.6 kJ/mol. However, when the ZPE is taken into account, the situation is reversed and the symmetrical η^2(H,H) structure is 0.6 kJ/mol lower in energy than the η^2(H,C) structure, leading to one shallow energy minimum rather than two minima separated by a small barrier. Nevertheless, it can be safely assumed that the rotation occurs essentially unhindered at the temperatures in question. This agrees with the observed multiple deuterium incorporation in the exchange experiments.

The η^2(H,C) and η^2(H,H) structures were further investigated by calculations of the energies of the DFT-optimized structures with various high-level ab initio methods using the Gaussian94 program[36] (vibrational frequencies were not calculated). The η^2-(H,C) structure was found to be most stable for all the methods used. In summary, the energy difference between η^2(H,C) and η^2(H,H) was calculated to be 0.6 kJ/mol (DFT) versus 1.2 (CCSD(T)), 1.6 (CCSD), 1.5 (MP4(SDQ)), 1.2 (MP2), and 2.7 (HF) kJ/mol. Thus, the η^2(H,C) bonding mode is found to be the most stable, excluding ZPE corrections, by a small margin in all cases.

The Pt−N bond distances trans to the ligand (or vacant site) in the cations (N-N)Pt$(CH_3)(L)^+$ (**A**−**D**) decrease by ca. 0.04 Å in the order CH_4 > H_2O ≈ TFE > vacant site according to the trans influence of the groups, whereas the cis Pt−N distance changes by only 0.01 Å. Methane, with a 99 kJ/mol bond to the (N-N)Pt$(CH_3)^+$ fragment, is a relatively poor ligand compared to H_2O (158 kJ/mol) and TFE (149 kJ/mol) according to the DFT calculations. It may therefore appear surprising that methane C−H activation occurs at all from the aqua complex. However, it must be borne in mind that in the real system in solution, the position of the ligand-exchange equilibria shown in Scheme 4 will depend not only on the relative ligand binding energies to Pt, but also on the solvation energies of the species involved. In particular, the relative solvation properties of H_2O, TFE, and CH_4 must play a major role. The small, strongly hydrogen-bonding molecules H_2O and TFE have significantly greater solvation energies in TFE than does CH_4, and this factor will counteract the trend of the Pt−ligand bond energies on the equilibria. A relatively small solvation energy for CH_4 in TFE may contribute significantly to increase the driving force, and to lower the activation barriers, for the substitution of CH_4 for H_2O and TFE at the Pt center, regardless of whether the exchange processes occur by associative or dissociative mechanisms.

Scheme 4

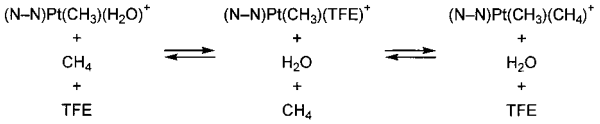

Five- and Six-Coordinate Oxidative Addition Products (N-N)Pt$(CH_3)_2$(H)(L)$^+$ (L = Vacant Site, H_2O, or TFE). Oxidative addition of methane within the σ-complex (N-N)Pt-$(CH_3)(\sigma$-$CH_4)^+$ may, in principle, occur to give the five-coordinate oxidative addition product (N-N)Pt$(CH_3)_2(H)^+$ with the hydride located either in an apical position (**E**) or in an equatorial position (**F**). If the latter is favored, then the principle of microscopic reversibility dictates that there must be an available pathway for the interchange of the two nonequivalent methyl groups for the Pt−CH_3/CH_4 exchange process. The DFT calculations show that the isomer with an apical hydride is the most stable of the two at an energy +23 kJ/mol relative to the σ-complex, compared to the isomer with the equatorial hydride at +29 kJ/mol. The same relative ordering of hydride-apical and hydride-equatorial energies was calculated (B3LYP) for *cis*-$(PH_3)_2Pt(Cl)(CH_3)_2(H)^+$, but with a smaller energy difference (+98 and +100 kJ/mol relative to the σ-complex, respectively).[29e] The hydride-apical isomer of $(H_2NCH_2CH_2NH_2)Pt(CH_3)_2(H)^+$ was located 7 kJ/mol higher in energy than the σ-complex including ZPE,[29f] and that of *cis*-$(NH_3)_2Pt(CH_3)_2(H)^+$ was 38 kJ/mol higher, ZPE apparently not included.[29a] From these results, the reaction energies for the oxidative addition reactions appear to be strongly dependent on the ancillary ligands of the complexes (although differences in computational methods and basis sets may account for parts of the differences). The reactions to yield the five-coordinate products are always uphill in energy from the σ-complexes.

The five-coordinate C−H oxidative addition products have never been directly observed, presumably because of the unfavorable thermodynamics of their formation relative to that of the precursors as well as a low barrier against reductive elimination. However, in one instance, a five-coordinate C−H oxidative addition product has been trapped by rapid intramolecular attachment of a pendant donor ligand. Wick and Goldberg[10] reported that treatment of $K^+[(\eta^2$-Tp′)Pt$(CH_3)_2]^-$ with $B(C_6F_5)_3$ in the presence of hydrocarbons R−H gave the stable octahedral complexes (η^3-Tp′)Pt(CH_3)(R)(H), presumably

(34) (a) Crabtree, R. H. *Angew. Chem., Int. Ed. Engl.* **1993**, *32*, 789. (b) Hall, C.; Perutz, R. N. *Chem. Rev.* **1996**, *96*, 3125.

(35) (a) Hall, C.; Perutz, R. N. *Chem. Rev.* **1996**, *96*, 3125. (b) Billups, W. E.; Chang, S.-C.; Hauge, R. H.; Margrave, J. L. *J. Am. Chem. Soc.* **1993**, *115*, 2039.

(36) Frisch, M. J.; Trucks, G. W.; Schlegel, H. B.; Gill, P. M. W.; Johnson, B. G.; Robb, M. A.; Cheeseman, J. R.; Keith, T.; Petersson, G. A.; Montgomery, J. A.; Raghavachari, K.; Al-Laham, M. A.; Zakrzewski, V. G.; Ortiz, J. V.; Foresman, J. B.; Cioslowski, J.; Stefanov, B. B.; Nanayakkara, A.; Challacombe, M.; Peng, C. Y.; Ayala, P. Y.; Chen, W.; Wong, M. W.; Andres, J. L.; Replogle, E. S.; Gomperts, R.; Martin, R. L.; Fox, D. J.; Binkley, J. S.; Defrees, D. J.; Baker, J.; Stewart, J. P.; Head-Gordon, M.; Gonzalez, C.; Pople, J. A. *Gaussian 94*, Revision D.4; Gaussian, Inc.: Pittsburgh, PA, 1995.

via C−H oxidative addition at a three-coordinate complex (η^2-Tp′)Pt(CH_3), followed by rapid intramolecular trapping by the pendant arm of the Tp′ ligand. Stable Pt(IV) hydridodialkyl complexes have been generated in other instances by protonation of four-coordinate dialkyl precursors. The hydridoalkyl complexes can be observed and sometimes even isolated if the sixth coordination site is occupied by a ligand that does not undergo facile dissociation, as found in complexes **8a** and **8b** in this work and previously reported by others.[9a,37] In those instances where bis(chelating) supporting ligands are present, the hydride ligand appears to always occupy an apical position relative to the chelate.[9a,37a,c,e,f,i]

The DFT calculations of (N-N)Pt$(CH_3)_2(H)^+$ (**E**; hydride apical) were supplemented by calculations for the six-coordinate complexes resulting from addition of a H_2O (**G**) or TFE (**H**) ligand at the second apical coordination site. Coordination of the two ligands to give hexacoordinate species resulted in a stabilization of the pentacoordinate oxidative addition products by 87 and 78 kJ/mol, respectively, ZPE not included. The H−Pt−CH_3 angles in **E**, **G**, and **H** remain rather invariant at 85°. This suggests that the tilt of the hydride toward the methyl group is not indicative of a significant residual H_3C−H bonding interaction. The NMR investigation of the (N^f-N^f)Pt$(CH_3)(H_2O)^+$ complex indicates that H_2O binds considerably better to the cationic Pt(II) center than does TFE. Our DFT calculations also established a stronger binding of L = H_2O relative to TFE in the Pt(II) complex (N-N)Pt$(CH_3)(L)^+$ as well as in the Pt(IV) oxidative addition products (N-N)Pt$(CH_3)_2(H)(L)^+$. The stabilization caused by H_2O relative to TFE was somewhat greater for the five-coordinate oxidative addition product than for the three-coordinate precursor.

Computational Search for an Oxidative Addition Mechanism for the Methane C−H Activation. The oxidative addition was investigated with the σ-complex **D** as the starting point. With the elongated C−H bond as the reaction coordinate, the calculations ultimately led to the Pt(IV) complex (N-N)Pt$(CH_3)_2(H)^+$ with the hydride in the apical position (**E**). The reaction and activation energies were found to be 23 and 33 kJ/mol, respectively. A complete exchange involves a reductive elimination following the reverse path compared to oxidative addition. In the transition state **I**, the Pt−H distance has decreased to 1.54 from 1.84 Å in **D**, the Pt−C distance decreased to 2.11 from 2.34 Å, and the C−H distance increased to 1.73 from 1.16 Å.

Interestingly, we were unable to locate a transition state that directly connects the σ-complex **D** and the Pt(IV) complex (N-N)Pt$(CH_3)_2(H)^+$, in which the hydride ligand occupies the *equatorial* position (**F**), even though **E** and **F** are essentially equally stable. We cannot safely rule out that the failure to find a reaction path that directly connects σ-complex **D** and the hydride-equatorial Pt(IV) complex **F** stems from the chosen reaction coordinate having an insufficient overlap with the lowest-energy path. The reaction was therefore investigated in the opposite direction, i.e., as the reductive elimination from **F** with the developing C−H bond as the reaction coordinate. The calculations showed that this reaction would occur via an initial interchange to the other isomer, **E**. This interchange occurs by a concerted motion of the apical methyl group and the equatorial hydride perpendicular to the equatorial plane in the five-coordinate species and has a calculated activation energy of 9 kJ/mol. The process is reminiscent of the one responsible for the interchange of basal and apical methyl groups in Ru($P^tBu_2Me)_2$(CO)Me_2.[38] The reductive elimination from **E** is now, of course, the microscopic reverse of the oxidative addition starting from **D**. These results somewhat contrast the DFT (B3LYP) results of Bartlett et al.[29e] on the hydride-apical and hydride-equatorial isomers of *cis*-$(PH_3)_2$Pt(Cl)$(CH_3)_2(H)^+$, both of which underwent elimination to yield the corresponding σ-complex through a common "pinched trigonal bipyramidal" transition state.

Reductive elimination of ethane from the Pt(IV) complex **E** was not investigated. Ethane formation is not experimentally observed, and such a process would probably have a much higher activation barrier than reductive elimination of methane.[29a,39]

Computational Search for a σ-Bond Metathesis Mechanism for the Methane C−H Activation. Starting from the σ-complex **D**, the distance between the most strongly interacting Pt-bonded hydrogen atom in methane and the Pt−CH_3 carbon atom was used as the reaction coordinate in the investigation of the σ-bond metathesis reaction. The use of this reaction coordinate offers the advantage that this C−H distance hardly changes in the oxidative addition reaction pathway, and hence is approximately orthogonal to the latter path. When this C−H distance was decreased, the reaction trajectory of an apparent σ-bond metathesis was obtained. However, in an attempt to trace the same reaction coordinate in reverse by increasing the C−H distance, an oxidative addition trajectory resulted. This hysteresis is likely an artifact[40] caused by the choice of a reaction coordinate for the methane elimination that diverges from the lowest-energy path of the reaction, and may be interpreted as an indication that the σ-bond metathesis mechanism is unlikely.

Hoping to investigate the σ-bond metathesis using a different reaction coordinate, we considered that the migrating hydrogen atom may be situated equidistant from the two C atoms when the transition state is reached because of the natural molecular symmetry of this state. Another possibility is that the hydrogen atom is located within the equatorial plane (this is confirmed by the calculations, vide infra). These geometry restrictions were achieved by imposing either molecular C_s symmetry by a mirror plane perpendicular to the equatorial plane, or C_2 symmetry by an axis through the midpoint of the diimine C−C bond and the Pt atom. Minimizing the energy with *either* of these symmetry restrictions gave a transition state **J** which has C_{2v} symmetry. The transition state has a single imaginary vibration frequency for the transfer of the hydrogen atom between the methyl groups. The calculations give an activation barrier of 44 kJ/mol for the σ-bond metathesis mechanism, to be compared with the previously found 33 kJ/mol for oxidative addition. The results are therefore slightly in favor of an oxidative addition pathway over σ-bond metathesis, but the difference of 11 kJ/mol is not large. It is clear that coordination of solvent molecules as well as bulk solvent effects could easily perturb the system sufficiently to even invert the trend. We therefore decided to explicitly include a solvent molecule in the calculations.

(37) (a) Hill, G. S.; Rendina, L. M.; Puddephatt, R. J. *Organometallics* **1995**, *14*, 4966. (b) O'Reilly, S. A.; White, P. S.; Templeton, J. L. *J. Am. Chem. Soc.* **1996**, *118*, 5684. (c) Hill, G. S.; Puddephatt, R. J. *J. Am. Chem. Soc.* **1996**, *118*, 8745. (d) Canty, A. J.; Dedieu, A.; Jin, H.; Milet, A.; Richmond, M. K. *Organometallics* **1996**, *15*, 2845. (e) Hill, G. S.; Vittal, J. J.; Puddephatt, R. J. *Organometallics* **1997**, *16*, 1209. (f) Jenkins, H. A.; Yap, G. P. A.; Puddephatt, R. J. *Organometallics* **1997**, *16*, 1946. (g) Canty, A. J.; Fritsche, S. D.; Jin, H.; Patel, J.; Skelton, B. W.; White, A. H. *Organometallics* **1997**, *16*, 2175. (h) Prokopchuk, E. M.; Jenkins, H. A.; Puddephatt, R. J. *Organometallics* **1999**, *18*, 2861. (i) Fekl, U.; Zahl, A.; van Eldik, R. *Organometallics* **1999**, *18*, 4156. (j) Haskel, A.; Keinan, E. *Organometallics* **1999**, *18*, 4677.

(38) Huang, D.; Streib, W. E.; Bollinger, J. C.; Caulton, K. G.; Winter, R. F.; Scheiring, T. *J. Am. Chem. Soc.* **1999**, *121*, 8087.

(39) Blomberg, M. R. A.; Siegbahn, P. E. M.; Nagashima, U.; Wennerberg, J. *J. Am. Chem. Soc.* **1991**, *113*, 424.

(40) Minkin, V. I.; Simkin, B. Ya.; Minyaev, R. M. *Quantum Chemistry of Organic Compounds*; Springer-Verlag: Berlin, 1990.

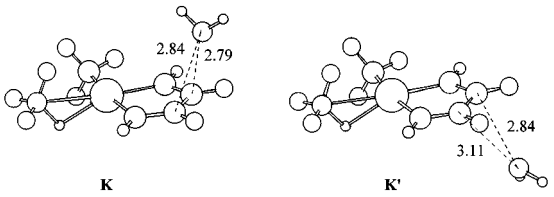

Figure 3. Association of a H_2O molecule at the diimine moiety of $(N\text{-}N)Pt(CH_3)(CH_4)^+$ in anti (**K**) and syn (**K′**) mode relative to the bridging H of the methane ligand.

Explicit Inclusion of a H_2O or TFE Molecule on the C−H Activation. Calculations including a solvent molecule were performed starting at the square planar $(N\text{-}N)Pt(CH_3)(CH_4)^+$ σ-complex **D**. All stationary points were reoptimized with an H_2O or TFE molecule attached. Several points of attachment for H_2O and TFE were tried in each case, and it was found that for the σ-complex as well as for the transition state of the σ-bond metathesis, the most stable structures contain the solvent molecule *associated at the C−C bond of the diimine*. In no cases were any minima located where the solvent molecule coordinates to the metal center in the σ-complex through the use of the O (or F for TFE) lone pairs or through hydrogen bonding between the solvent oxygen and the Pt-bonded hydrogen atom of the methane ligand.[41] The calculated lowest-energy structure of $H_2O\cdot(N\text{-}N)Pt(CH_3)(CH_4)^+$ (**K**) has the H_2O molecule located on the opposite side of the Pt−diimine plane with respect to the Pt-bonded H of the methane ligand. A structure with methane-H and H_2O on the same side of the plane was also found (**K′**), at a local energy minimum only 1 kJ/mol higher in energy. The structures of **K** and **K′** are depicted in Figure 3. A similar situation pertained to TFE (**L** and **L′**, respectively; in this case **L** was less stable than **L′** by 6 kJ/mol).

The calculations showed that H_2O and TFE association at the C−C bond of diimine occurs mostly through an electrostatic attraction (calculated Mulliken charges are +0.3 at the diimine carbon atoms, and −0.6 and −0.7 at oxygen from H_2O and TFE, respectively). This situation is fairly general for the cationic (N-N)Pt complexes, for which calculations were performed with H_2O or TFE present. In this context, it is interesting to note that a $^{19}F\{^1H\}$ HOESY NMR investigation of (diimine)Pt-(CH_3)(alkene)$^+BF_4^-$ ion pairs in dichloromethane-d_2 indicated that the BF_4^- counteranion is associated with the cation near the diimine moiety.[42] The binding energies between H_2O and the diimine C−C bond were calculated for several Pt complexes: $H_2O\cdot(N\text{-}N)Pt(CH_3)(CH_4)^+$ (**K**), 30 kJ/mol; **K′**, 29 kJ/mol; $H_2O\cdot(N\text{-}N)Pt(CH_3)_2(H)^+$, 32 kJ/mol; transition state for σ-bond metathesis, 28 kJ/mol. For TFE binding, the data were, for $TFE\cdot(N\text{-}N)Pt(CH_3)(CH_4)^+$ (**L**), 21 kJ/mol; **L′**, 27 kJ/mol; $TFE\cdot(N\text{-}N)Pt(CH_3)_2(H)^+$, 28 kJ/mol; transition state for σ-bond metathesis, 27 kJ/mol. Nonsolvent zero-point energies are not included in these bond energies, as the correction does not contribute to the bond energy of solvent binding to the diimine. The minimum energy structures of species containing TFE were not verified by vibrational frequency calculations, due to their extensive size. The non-ZPE-corrected energies are included in Table 2. In addition, a relatively simple *partial* ZPE correction was applied to the calculated energies for the solvent-associated species: it was assumed that the same ZPE correction applies to solvent-associated species as to the corresponding species without solvents. This results in the *estimated* ZPE-corrected data that are also listed in Table 2.

To further probe the effects of coordinated or associated solvent molecules, we wanted to estimate the energy change when TFE is solvated rather than bonded to the Pt complex. Whether TFE is bonded at Pt or diimine or is in solution, the CF_3CH_2 tail of TFE will interact with adjacent TFE solvent molecules. The main contribution to the difference between coordinated and solvated TFE will be the bond between the TFE hydroxyl group and either Pt, diimine, or TFE. Calculations on various $(TFE)_n$ ($n = 2-5$) clusters indeed showed that the strongest TFE−TFE interaction was of the O−H···O type. The interaction was calculated as the average energy lost per hydrogen bond when the TFE cluster was dissociated into separate molecules at infinite distance.[43] The strongest hydrogen bond was found to be 31 kJ/mol for a TFE pentamer.[44] We have already described that a TFE molecule interacts with the diimine C−C bond with 28 kJ/mol or less in all calculated structures, so it appears that the energy involved is approximately the same whether a TFE molecule binds to the diimine or to the TFE solvent. TFE association/dissociation must occur rapidly under the C−H activation conditions.

The influence of H_2O on the activation barrier for the oxidative addition process was probed by investigating its microscopic reverse. The search for the transition state for the reductive elimination was attempted, starting from the octahedral Pt(IV) complex $(N\text{-}N)Pt(CH_3)_2(H)(H_2O)^+$ (**G**). The H−Pt−C(methyl) angle was used as the reaction coordinate. The H_2O ligand was found to depart from the Pt center during the reductive elimination, and at the stage when a σ-complex was formed, the H_2O had reattached itself at the diimine C−C bond. We were not entirely successful at locating the exact transition state. Two imaginary frequencies were calculated, one large that corresponds to the C−H bond formation, and one very small ($9i$ cm^{-1}) that involves a twist movement of coordinated H_2O around the long and flexible Pt−O bond. Since the Pt−O bond has been elongated by 0.50 Å relative to in **G**, this twisting movement should give only a negligible contribution to the energy, and the energy of this structure (**M**) should be very close to that of the true transition state. Further movement along the chosen reaction coordinate gave the σ-complex **K** with H_2O associated at the diimine C−C bond, on the opposite side of the Pt−diimine plane relative to the Pt-bonded H atom of coordinated methane. The calculated activation energy of oxidative addition is 27 kJ/mol, and the reaction energy is −33 kJ/mol.

The effect of including a water molecule on the σ-bond metathesis mechanism was also attempted. The σ-bond metathesis could not be investigated the same way as for the nonsolvent case because inclusion of H_2O removed all symmetry. This prevented optimization with symmetry restrictions, in contrast to the optimization of the σ-bond metathesis with no solvent. The σ-bond metathesis pathway was explored instead by attaching H_2O to different sites of the frozen structure of the nonsolvent transition state. It was found that the added

(41) Hydrogen bonds between transition metal hydrides and proton donors such as O−H and N−H have recently been reported. For a review, see: Crabtree, R. H.; Siegbahn, P. E. M.; Eisenstein, O.; Rheingold, A. L.; Koetzle, T. F. *Acc. Chem. Res.* **1996**, *29*, 348.

(42) Zuccaccia, M.; Macchioni, A.; Orabona, I.; Ruffo, F. *Organometallics* **1999**, *18*, 4367.

(43) The maximum number of hydrogen bonds was obtained by placing the molecules in a circle such that the overlap between H and a lone pair of O was optimal for all hydrogen bonds. Binding energies were calculated for several $(TFE)_n$ clusters, and the largest energies obtained per hydrogen bond for each oligomer were $n = 2$, 19 kJ/mol; $n = 4$, 27 kJ/mol; $n = 5$, 31 kJ/mol. The last value is used as the estimate for the energy that is gained when the O−H group of TFE binds to the solvent.

(44) Although comparisons are not directly relevant, it is interesting to note that the experimentally determined heat of vaporization of TFE is $\Delta H° = 44$ kJ/mol: Rochester, C. H.; Symonds, J. R. *J. Chem. Soc., Faraday Trans. 1* **1973**, *69*, 1267.

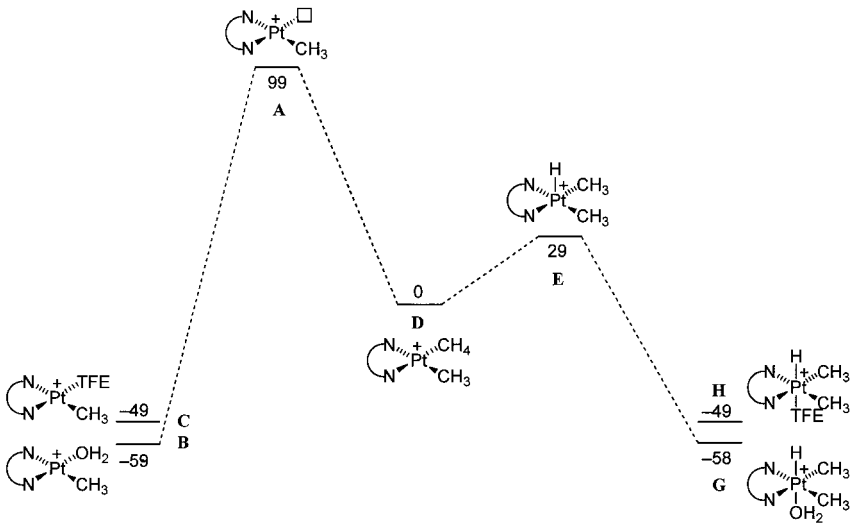

Figure 4. Energy diagram depicting ground-state structures in the C−H activation of methane. All energies are in kilojoules per mole relative to the σ-complex **D**, and ZPE corrections are not included.[31]

solvent molecule was preferentially associated at the diimine C−C bond. The H_2O−diimine bond strength was essentially unchanged (a 2 kJ/mol weakening) when compared to that of the starting σ-complex. No energy minimum was located in which H_2O coordinates at the Pt atom of the frozen transition-state structure for the σ-bond metathesis, and no evidence for hydrogen bonding between H_2O and the migrating H atom (Mulliken charge of −0.1) was found.[41] Thus, short-range interactions with a H_2O molecule appear to have little effect on the energy barrier for the σ-bond metathesis.

The influence of TFE on the activation barrier for the oxidative addition process was also probed by investigating its microscopic reverse starting from **H**. The distance between the hydride and the methyl carbon atom was used as the reaction coordinate and was decreased until a methane σ-complex was formed. The results were quite similar to those just described with H_2O included. The TFE ligand departed from the metal and reattached itself to the molecule at the diimine. This is entirely consistent with the previously found tendency for TFE to interact with the diimine part of the σ-complex. The attempts at locating the exact transition state for this reductive elimination were again not entirely successful. Two imaginary frequencies were calculated, one large that corresponds to the C−H bond formation and a second, small one ($32i$ cm^{-1}) that could not be eliminated. In the mode corresponding to the latter, the TFE molecule moves sideways without affecting Pt−O bond length. The Pt−O bond is elongated by 0.54 Å relative to the minimum in the oxidative addition product **H** and is therefore very flexible. This fact, as well as the imaginary frequency being so small, makes it reasonable to assume that the energy of this structure (**N**) is close to that of the true transition state. This gives an approximate activation energy of 56 kJ/mol for the reductive elimination and 22 kJ/mol for the reverse, the oxidative addition.

Finally, the σ-bond metathesis pathway was explored by attaching TFE to different sites of the frozen structure of the nonsolvent transition state. The results paralleled those found when H_2O was included. As for the σ-complex, TFE would attach only to the diimine group, with similar bond strengths in both the frozen nonsolvent σ-bond metathesis transition state and in the σ-complex **L**.

Mechanistic Consequences of the Computational Results. Figure 4 summarizes some calculated data (non-ZPE data from Table 2, since these give the most complete diagram) of ground-state species that are likely to be involved in the C−H activation process. Under actual reaction conditions, $(N^f\text{-}N^f)Pt(CH_3)(H_2O)^+$ is the only observable complex in solution, and this is consistent with **B** being of lowest energy. No evidence has been found for the coexistence in solution of $(N^f\text{-}N^f)Pt(CH_3)(TFE)^+$, modeled by **C**, although an equilibrium between H_2O and TFE adducts has been observed and quantified in a related system.[24] The proposed intermediate σ-complex **D** that is crucial to explain the occurrence of multiple H/D exchange between Pt−CH_3 and CD_4 is located 59 kJ/mol higher in energy than the aqua complex **B**. The σ-complex may be accessed by a preequilibrium dissociation of H_2O from **B** to give the three-coordinate species **A**, 158 kJ/mol higher in energy than **B**. The dissociation of H_2O, experimentally hinted at by the partial inhibition of the reaction caused by addition of water, will significantly contribute to the overall barrier of the reaction if **A** is involved.[45] The five-coordinate complex **E** is 29 kJ/mol uphill from the σ-complex, but coordination of a second axial ligand H_2O or TFE renders the formation of the six-coordinate oxidative addition products **G** or **H** more favorable. In fact, the six-coordinate products **G** and **H** are essentially of the same energy as the starting complexes **B** and **C**, respectively. However, entropy effects are not included and will render the overall reactions to give **G** or **H** less favorable by ca. 45 kJ/mol under ambient conditions.[46] The relatively high stability predicted for **G** is reconciled with the fact that hydridoalkyl complexes $(N^f\text{-}N^f)Pt(CH_3)_2(H)(L)^+$ (**8a**,**b**) were observable at low temperatures in dichloromethane-d_2. The methane σ-complex has not been observed under the actual reaction conditions, and this is readily understood considering that **D** is much higher in energy than **B** or **G** and therefore must have a short lifetime under reaction conditions where it is thermally generated from **B** or **G**.

Calculated data for the reactions with and without H_2O and TFE association are summarized in Table 4. Figure 5 depicts energy diagrams for the oxidative addition and σ-bond metathesis pathways for the methane C−H activation reaction. To the left, the ZPE-corrected results of the nonsolvent calculations

(45) The calculated 158 kJ/mol barrier is considerably larger than that implicated by the experimental observations (the Eyring equation yields a free energy of activation of ca. 110 kJ/mol when a rate constant corresponding to a half-life of 48 h at 45 °C is used). This may be another hint that an associative mechanism for methane coordination should be seriously considered. We hope to address this point in a future contribution.

(46) (a) Page, M. I. *Angew. Chem., Int. Ed. Engl.* **1977**, *16*, 449. (b) Nolan, S. P.; Hoff, C. D.; Stoutland, P. O.; Newman, L. J.; Buchanan, J. M.; Bergman, R. G.; Yang, G. K.; Peters, K. S. *J. Am. Chem. Soc.* **1987**, *109*, 3143.

Table 4. Relative Energies, kJ/mol

	solvent			
	none, ZPE-corrected[a]	none, not ZPE-corrected[a]	TFE, partially ZPE-corrected[b]	H_2O, partially ZPE-corrected[b]
σ-complex (CH_4)	0	0	−27	−30
oxidative addition transition state	33	40	2	−4
oxidative addition product	23	29	−55	−64
σ-bond metathesis transition state	44	50	17	16

[a] From Table 2. [b] Obtained by applying a partial ZPE correction to the solvent-associated species. The partial correction amounts to the ZPE correction that was applied to the corresponding solvent-free species (**D**, **E**, **I**, **J**) in Table 2 and simply equals the difference between ZPE and non-ZPE-corrected values in Table 2.

are illustrated. The oxidative addition to form the five-coordinate complex **E** is 23 kJ/mol uphill in energy with activation barriers of 33 kJ/mol for the oxidative addition and 10 kJ/mol for the reverse. The σ-bond metathesis exchange reaction has an activation barrier of 44 kJ/mol and is therefore disfavored by 11 kJ/mol relative to oxidative addition.

This preference is retained but somewhat modified when a molecule of H_2O is included in the calculations. These calculations, as already mentioned, were done without ZPE corrections. A partial ZPE correction may, however, be applied; see footnote *b* to Table 4. The H_2O molecule associates at the diimine moiety of **D** and **J** involved in the σ-bond metathesis mechanism with the same binding energy of 28−30 kJ/mol. This lowers the ground-state and transition-state energies to approximately the same extent, and therefore, *no essential change in the activation energy is found for the σ-bond metathesis*. Contrasting this, the interaction of H_2O with the oxidative addition product **E** through axial coordination is much greater (87 kJ/mol), leading to considerable stabilization of the product **G**. The transition state for the oxidative addition, **N**, contains a considerably weakened (by ca. 0.5 Å) Pt−OH_2 bond. Here, the transition-state energy is lowered by 36 kJ/mol relative to the situation where H_2O coordination or association was not included. The activation barrier for oxidative addition is reduced to 27 kJ/mol (from 33 kJ/mol without H_2O), and for the reductive elimination it has *increased* from 10 to 60 kJ/mol as a consequence of the thermodynamic stabilization of the oxidative addition product by H_2O coordination. The preference for oxidative addition over σ-bond metathesis for the exchange process has increased from 11 to 20 kJ/mol. For TFE, the preference for oxidative addition amounts to 16 kJ/mol.

A large body of experimental evidence[47] suggests that C−H and C−C reductive eliminations from six-coordinate Pt(IV) complexes normally proceed with prior ligand dissociation so that the actual elimination occurs from a five-coordinate intermediate. This has been recently supported by DFT calculations.[29e] Attempts to computationally induce reductive elimination of methane from three isomers of $(PH_3)_2PtCl_2(CH_3)(H)$, all with cis phosphines and with the methyl and hydride ligands cis disposed, caused concomitant loss of the ligand that was trans to the hydride. For two isomers, forcing H and CH_3 together led to a monotonic increase in energy with concomitant PH_3 ejection. For the isomer with a trans (relative to H) chloride, bringing H and CH_3 together led to chloride dissociation, but in this case the energy did not increase monotonically—in fact, a transition state for the simultaneous methane elimination and chloride dissociation was located in which the Pt−Cl distance had increased by 0.26 Å compared to the ground-state distance. The 82 kJ/mol barrier for this reaction was dramatically greater than the 4 kJ/mol barrier toward elimination from the corresponding five-coordinate complex that results from removal of the chloride trans to hydride. The 78 kJ/mol energy difference, of course, does not take into account the significant but unreported energy cost of chloride predissociation that is needed when the six-coordinate complex is the starting point. Siegbahn and Crabtree[29b] also found that methane elimination with concomitant ligand dissociation occurred from $(H_2O)_2PtCl_2(CH_3)(H)$.

Interestingly, our calculations suggest a pathway for the reductive elimination from **G** with a transition state **M** in which the H_2O ligand is incompletely dissociated from the Pt center in the six-coordinate complex. This behavior parallels the chloride dissociation from one of the three isomers of $(PH_3)_2PtCl_2(CH_3)(H)$, as mentioned above. The 60 kJ/mol energy barrier for the elimination from **G** via **M** is considerably greater than the 10 kJ/mol barrier from **E** via **I** (Figure 5). However, due to the 87 kJ/mol energy cost of a predissociation of H_2O from **G**, the concerted elimination/dissociation (**G**−**M**−**K**) will have a lower overall barrier, by 36 kJ/mol, than a two-step elimination (**G**−**E**−**I**−**D**). An attractive interaction between the diimine moiety and the departing H_2O in the transition state presumably contributes to this effect.

Concluding Remarks. We have demonstrated that a cationic Pt(II) diimine complex is capable of activating benzene and methane C−H bonds under mild conditions. These reactions proceed in the hydroxylic solvent TFE, and in the presence of substantial quantities of water—a potential ligand that is usually excluded from the reaction media for such reactions. Multiple H/D exchanges between coordinated CH_3 groups and C_6D_6 or CD_4 imply the intermediacy of methane σ- and benzene σ- or π-complexes. Theoretical calculations suggest that an oxidative addition pathway is favored over a σ-bond metathesis alternative for the methane C−H activation. Single water or TFE molecules associate with the involved complexes preferentially at the diimine moiety of square planar Pt(II) species and at a vacant apical site of square pyramidal Pt(IV) species. The thermodynamics and kinetics of C−H bond formation from Pt(IV) and of C−H bond cleavage from Pt(II) methane σ-complexes show a pronounced dependence on whether water or TFE is present or not.

Experimental Section

General Considerations. Acetonitrile was distilled from P_2O_5, and dichloromethane and dichloromethane-d_2 were distilled from CaH_2. Trifluoroethanol (TFE) and TFE-d_3 were distilled from $CaSO_4$ and a small amount of $NaHCO_3$. ^1H, $^{13}C\{^1H\}$, and ^{19}F NMR spectra were recorded on Bruker Advance DXP 200 and 300 instruments.

^1H and ^{13}C chemical shifts are reported in ppm relative to tetramethylsilane, with the residual solvent proton resonance as internal standards. ^{19}F chemical shifts are reported in ppm relative to $CFCl_3$. For TFE-d_3, the solvent fluorine resonance was used as internal standard (δ −77.72). Elemental analyses were performed by Ilse Beetz Mikroanalytisches Laboratorium, Kronach, Germany. $Pt(CH_3)_4(\mu\text{-}SMe_2)_2$[15] and $Pt(C_6H_5)_2(SMe_2)_2$[16] were prepared as described in the literature.

The following compounds were prepared as described in the Supporting Information to ref 13: N^t-N^r, **1**, **2**, **3**(BF_4^-), **4**(BF_4^-), and **6**(BF_4^-).

(47) Crumpton, D. M.; Goldberg, K. I. *J. Am. Chem. Soc.* **2000**, *122*, 962 and references cited, as well as refs 14 and 15 cited in ref 29e.

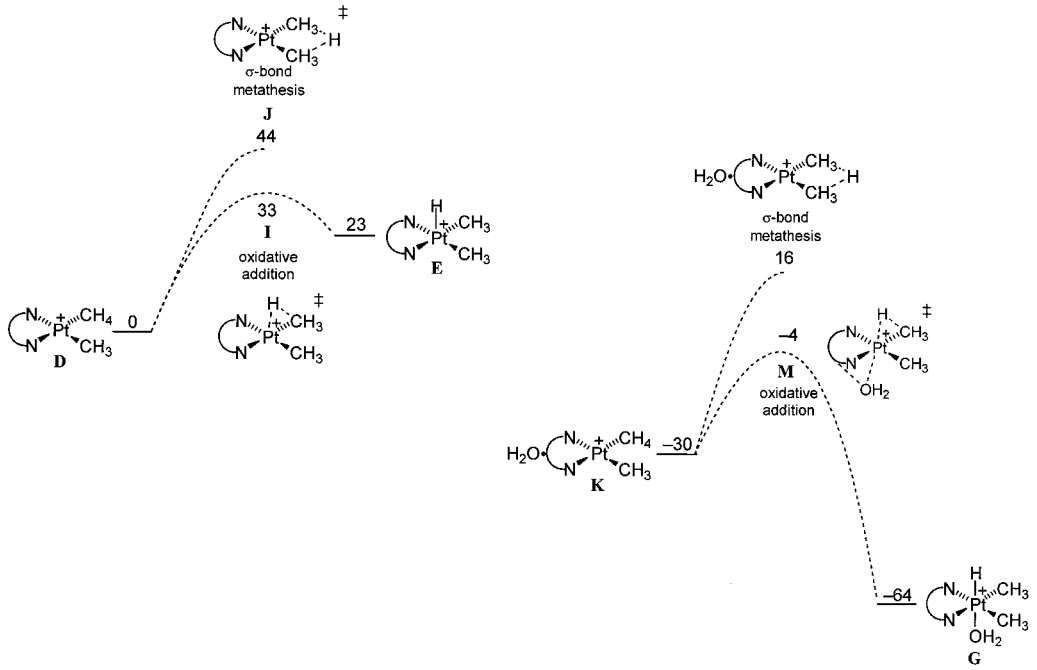

Figure 5. Energy diagram (kJ/mol) depicting the C−H activation step following oxidative addition and σ-bond metathesis pathways. Left, no H_2O included; ZPE-corrected values. Right, one H_2O molecule included; partial ZPE correction applied as explained in footnote *b* to Table 4.

Attempted Preparation of (N^f-N^f)Pt(CH_3)(OTf) (5). A −40 °C solution of **1** (24.1 mg, 3.29×10^{-2} mmol) in dichloromethane (10 mL) was added HOTf (2.9 μL, 3.3×10^{-2} mmol), and the reaction mixture was stirred for 15 min. The solvent was slowly removed by vacuum transfer, while the solution was maintained at −40 °C. The residue was dried in vacuo at ambient temperature to give an orange powder. NMR analysis immediately after dissolving the material in dichloromethane-d_2 showed that **5** is the major product formed in the reaction (ca. 90%). ^{1}H NMR (200 MHz, dichloromethane-d_2): δ 1.07 (s, $^2J(^{195}\text{Pt}-\text{H}) = 74.9$ Hz, 3 H, Pt*Me*), 1.65 (s, $^4J(^{195}\text{Pt}-\text{H}) = 13.1$ Hz, 3 H, NC*Me*C′MeN), 2.01 (s, 3 H, PtNC*Me*), 2.13 (s, 3 H, NCMeC′*Me*N), 7.62 (s, 2 H, ArH_o), 7.71 (s, 2 H, Ar′H_o), 7.96 (s, 1 H, ArH_p), 8.01 (s, 1 H, Ar′H_p). ^{19}F NMR (188 MHz, dichloromethane-d_2): δ −78.48 (s, $^4J(^{195}\text{Pt}-\text{F}) = 14.5$ Hz, 3 F, BF_4^-), −63.47 (s, 6 F, ArCF_3), −63.36 (s, 6 F, Ar′CF_3). Compound **5** decomposes in dichloromethane over time, and after a period of 62 h the signals for **5** had decreased to ca. one-third of their original intensities. The degradation of **5** is accompanied by precipitation of brown, unidentified material and formation of CH_4.

C−H Activation of Benzene and Formation of 7(BF_4^-). To a solution of **6**(BF_4^-) (6.8 mg, 8.3×10^{-3} mmol) in TFE-d_3 (0.6 mL) in an NMR tube was added benzene (22 μL, 0.25 mmol). The reaction was monitored by ^{1}H and ^{19}F NMR spectroscopies. A smooth conversion of **6** to the phenyl analogue [(N^f-N^f)Pt(C_6H_5)(OH_2)]$^+$ (**7**) was observed, with concomitant formation of CH_4, detected by ^{1}H NMR (δ 0.14). Spectroscopic data for **7**(BF_4^-) follow. ^{1}H NMR (200 MHz, TFE-d_3): δ 1.91 (s, 3 H, NC*Me*C′MeN), 2.19 (s, 3 H, NCMeC′*Me*N), 6.65−6.85 (m, 5 H, Pt−C_6H_5), 7.29 (s, 2 H, ArH_o), 7.65 (s, 1 H, ArH_p), 7.79 (s, 2 H, Ar′H_o), 8.05 (s, 1 H, Ar′H_p). ^{19}F NMR (188 MHz, TFE-d_3): δ −151.95 (s, 4 F, BF_4^-), −63.65 (s, 6 F, ArCF_3), −63.48 (s, 6 F, Ar′CF_3).

C−H Activation of CH_4 and CD_4. In a typical experiment, **6**(BF_4^-) dissolved in TFE-d_3 (0.4 mL) was placed in a high-pressure NMR tube. A known amount of methane (corresponding to 20−25 bar at ambient temperature) was condensed into the NMR tube. The tube was sealed and placed in a oil bath at 45 °C. The reactions were monitored by ^{1}H NMR.

Generation of (N^f-N^f)PtMe_2(H)(L)$^+$(BF_4^-) (8a(BF_4^-) and 8b(BF_4^-)) at −78 °C. To an NMR tube loaded with a solution of **1** (2.7 mg, 3.7×10^{-3} mmol) in dichloromethane-d_2 (400 μL) was slowly added dichloromethane-d_2 (100 μL) to form a separate upper layer. After subsequent slow addition of a mixture of 54% solution of HBF_4 in ether (1.0 μL, 7.3×10^{-3} mmol) in a mixture of dichloromethane-d_2 (100 μL) and diethyl ether (40 μL), the tube was sealed and cooled to −78 °C. The tube was shaken in order to mix the reactants (care was taken to minimize any heating of the sample), and a pale yellow solution was immediately obtained. The tube was then transferred to a precooled NMR probe. ^{1}H NMR (300 MHz, −55 °C), for **8a** (65%): δ −26.67 (s, $^1J(^{195}\text{Pt}-\text{H}) = 1741$ Hz, 1 H, Pt*H*), 0.54 (s, $^2J(^{195}\text{Pt}-\text{H}) = 63.6$ Hz, 6 H, Pt*Me*), 2.42 (s, 6 H, NC*Me*C*Me*N), 7.36 (s, 2 H, ArH_p), 7.92 (s, 4 H, ArH_o). ^{1}H NMR (300 MHz, −55 °C), for **8b** (35%): δ −26.40 (s, $^1J(^{195}\text{Pt}-\text{H}) = 1699$ Hz, 1 H, Pt*H*), 0.48 (s, $^2J(^{195}\text{Pt}-\text{H}) = 62.9$ Hz, 6 H, Pt*Me*), 2.37 (s, 6 H, NC*Me*C*Me*N), 7.36 (s, 2 H, ArH_p), 7.71 (s, 4 H, ArH_o). At temperatures above ca. −40 °C, the species **8a** and **8b** decompose under elimination of methane to give unidentified products. No other species could be observed prior to methane loss.

Theoretical Methods and Software. The geometries of all Pt complexes were optimized with density functional theory (DFT) using the ADF[48] program on a Cray T3E computer at the Norwegian University of Science and Technology, Trondheim, and on a HP V2500 computer at the University of Tromsø. The ab initio CCSD(T) calculations were performed with Gaussian94[36] on a Cray Origin 2000 computer at the High Performance Computer Center at the University of Bergen.

Slater exchange and the VWN parametrization of the LDA correlation energy were used,[49] with the gradient corrections of Becke[50] for exchange and of Perdew[51] for correlation (BP86). The gradient corrections were added self-consistently. The frozen core approximation was used for all atoms except hydrogen. The orbitals up to 4f and 1s were frozen in their atomic shapes for Pt and first-row atoms, respectively. The basis sets have the overall quality of TZV for Pt and DZVP for the other atoms. (We find that frozen 5p orbitals for Pt give

(48) ADF 2.3.0, Theoretical Chemistry, Vrije Universiteit, Amsterdam. (a) Baerends, E. J.; Ellis, D. E.; Ros, P. *Chem. Phys.* **1973**, *2*, 41. (b) te Velde, G.; Baerends, E. J. *J. Comput. Phys.* **1992**, *99*, 84. (c) Fonseca Guerra, C.; Visser, O.; Snijders, J. G.; te Velde, G.; Baerends, E. J. In *Methods and Techniques for Computational Chemistry*, METECC-95; Clementi, E., Coronglu, G., Eds.; STEF: Cagliari, 1995; pp 303−395.

(49) Vosko, S. H.; Wilk, L.; Nusair, M. *Can. J. Phys.* **1980**, *58*, 1200.

(50) (a) Becke, A. D. *Phys. Rev. A* **1988**, *33*, 2786. (b) Becke, A. D. In *The Challenge of d and f Electrons: Theory and Computation*; Salahub, D. R, Zerner, M. C., Eds.; ACS Symposium Series 394; American Chemical Society: Washington, DC, 1989. (c) Becke, A. D. *Int. J. Quantum Chem.* **1989**, *S23*, 599. (d) Becke, A. D. *Phys. Rev. A* **1988**, *38*, 2398.

(51) Perdew, J. P. *Phys. Rev. B* **1986**, *33*, 8822; *Phys. Rev. B.* **1986**, *34*, 7406 (erratum).

excellent bond lengths for Pt−H and Pt−C, but the calculated Pt−N bond lengths are too long by ca. 0.15 Å for the N to Pt.)

The stationary points of the model complexes within the nonsolvent approximation were characterized by calculating the vibrational spectrum, showing one and only one imaginary frequency for transition states and no imaginary frequency for energy minima, unless otherwise stated. Frequencies were computed in ADF by numerical differentiation of energy gradients in slightly displaced geometries. Each gradient was based on the gradient at the equilibrium and the gradients of two displaced geometries. The accuracy of the numerical integration for vibrational calculations was set to $10^{-6.5}$. For geometry optimizations it was set to $10^{-5.0}$ or higher accuracy when necessary, to converge the geometry.

The ab initio calculations were performed with Gaussian94.[36] The basis set for Pt was a modified version of Gaussian 94's LANL2DZ basis, which was extended through decontraction of the s and p shells to triple-ζ, and by addition of an extra uncontracted *d*-function with exponent 0.0457. The number of contracted valence basis functions, in order of increasing angular momentum, is (4,4,3). The basis set 6-31G(d,p) was used for all the other atoms.

Testing Model Systems for Calculations. It was necessary to model the reaction mechanisms with Pt complexes having a simpler diimine ligand X−N═C(Y)−C(Y)═N−X than in the experiments. Six model systems were considered: X = CH═CH_2, CH_3, or H, and Y = CH_3 or H. Calculated reaction energies for four relevant reactions were compared for the models with different diimine ligands, as well as for the full-sized Pt complex. The following test reactions were used.

$$(\text{diimine})\text{PtMe}^+ + \text{CH}_4 \rightarrow \textit{ax}\text{-}(\text{diimine})\text{PtMe}_2\text{H}^+$$

$$(\text{diimine})\text{PtMe}^+ + \text{CH}_4 \rightarrow \textit{eq}\text{-}(\text{diimine})\text{PtMe}_2\text{H}^+$$

$$(\text{diimine})\text{PtMe}(\text{OOCCF}_3) + \text{CH}_4 \rightarrow (\text{diimine})\text{PtMe}_2 + \text{CF}_3\text{COOH}$$

$$(\text{diimine})\text{PtMe}(\text{OSO}_2\text{CF}_3) + \text{CH}_4 \rightarrow (\text{diimine})\text{PtMe}_2 + \text{HOSO}_2\text{CF}_3$$

Acknowledgment. We gratefully acknowledge generous support from the Norwegian Research Council, NFR (stipends to L.J. and H.H. as well as computational time), and from Statoil under the VISTA program, administered by the Norwegian Academy of Science and Letters. We thank Aud M. Bouzga for kind assistance with some NMR experiments and Ulf Wahlgren for helpful discussions.

JA0019171